Coiled-coil mediated liposomal fusion: Asymmetric behaving peptide fusogens

Daudey, G.A.

CHAPTER V

LIPOSOME FUSION WITH ORTHOGONAL COILED-COIL PEPTIDES AS FUSOGENS: PEPTIDE ROLEPLAY IS CRITICAL FOR EFFICIENT FUSION

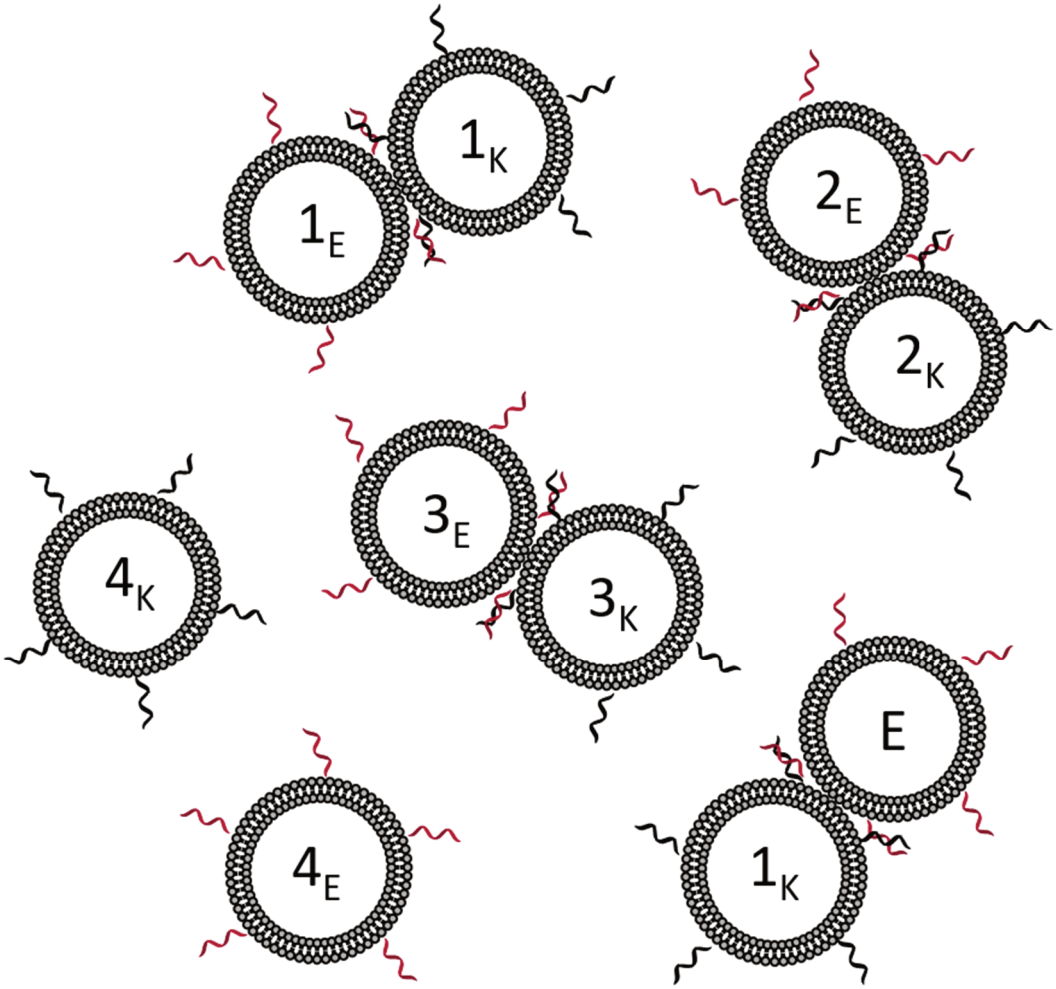

ABSTRACT

Biological membrane fusion is a highly specific and coordinated process, with multiple different vesicular fusion events proceeding simultaneously in the complex environment of a cell. Specific molecular recognition between transport vesicles and target membranes is established by various proteins, mostly belonging to the SNARE family of proteins, with minimal recognition between non-complementary proteins to avoid non-targeted fusion events. Here, specific recognition is introduced to a liposomal fusion model system by using lipidated derivatives of a set of four *de novo* designed heterodimeric coiled-coil peptide pairs. Content mixing of liposomes was only obtained between liposomes functionalized with complementary peptides, demonstrating the fusogenic activity of various coiled-coil peptides in general. The used peptide fusogens differ in coiled-coil binding affinities and peptide-membrane interactions which allowed us to study the relationship of the peptide characteristics and the efficiency of the fusion process. It was found that peptide-membrane interactions enhanced the fusion process, especially when the affinity between complementary peptides was relatively low. Furthermore, a new coiled-coil pair ($E/1_K$) was discovered, which was demonstrated to be an efficient fusogen together with coiled-coil pairs $2_E/2_K$ and $3_E/3_K$. These results will have broad implications for drug delivery systems by enabling targeted delivery of different carrier vesicles at various peptide-functionalized locations.

INTRODUCTION

Artificial membrane fusion is a steadily expanding field which allows the exploration of drug delivery systems and the study of cellular transport. In the last two decades, a variety of model systems were developed using phospho-lipid mimics of biological membranes with DNA,[1-9] peptides,[10-13] or small molecules[14-20] acting as fusogens. Most model systems are based on single complementary recognition units,[21] and thus are a limited mimic of the specific fusion events occurring in nature.[22-23] In cells, multiple different 'cargo vesicles' are transported to and delivered at precise locations in a complex environment, mainly mediated by the well-conserved class of SNARE-proteins.[24-25] Therefore, the ability to mimic the specificity of biological membrane fusion is the next challenge in the field of artificial membrane fusion. This would enable future drug delivery applications by enabling the development of simultaneous and/or site-specific fusion events.

Recently, the Vogel group achieved specific recognition with DNA based fusogens in a three-step liposomal fusion cascade.[8] However, their model system showed only efficient fusion at 50 °C, making their approach unsuitable for biological application. Our efforts in liposome fusion with the lipidated heterodimeric coiled-coil pair E and K (amino acid sequence $(EIAALEK)_3$ and $(KIAALKE)_3$ showed that lipidated coiled-coil peptides can mediate the fusion of liposomes in biological environments. Lipidation of peptides enables the insertion of these conjugates in liposomal membranes. Therefore, specific recognition in a liposomal fusion model system at biologically relevant temperatures could be achieved by using lipidated derivatives of orthogonal coiled-coil peptides. In recent years sets of orthogonal heterodimeric coiled-coil peptides became available via *de novo* peptide design.[26-31] These peptide pairs are able to form coiled-coils exclusively with their cognate partner while interactions with other (coiled-coil) peptides and homo-interactions are negligible.

Several orthogonal sets of heterodimeric coiled-coil peptides have been designed to date.[32-37] Although selective coiled-coil binding was demonstrated for all these sets of complementary peptides, they have to meet additional requirements to be useful candidates for peptide mediated fusion systems. Firstly, the coiled-coil peptides should interact at temperatures up to at least 30 °C to be applicable as fusogens at biologically

relevant temperatures, which is not the case for several sets of peptides developed by de groups of Aili and Woolfson.[32, 36-37] Also, the candidate peptides should not bind to biological targets to avoid unintended interactions, as could be the case with the set of coiled-coil peptides derived from Leucine peptide zipper DNA binding peptides.[35] The maximum number of potential pairs developed by Kennan was limited to 3 pairs due to a minimalistic approach using 3 heptad repeat peptides only.[33] Recently, this issue was solved by using 4 heptad repeat peptides (dubbed here P_E/P_K with P = 1 - 4). Elongation of the peptide sequence increased the coiled-coil stability (Tm > 40 °C) and the number of orthogonal pairs of coiled-coil peptides to four,[34] making these peptides useful candidates to be considered as fusogens in a partner specific liposomal fusion system.

Membrane conjugation of coiled-coil peptides can result in a change in the adopted conformation, oligomerization state or membrane interaction resulting in stabilized α-helical structures depending on their amphipathicity.[38-39] For the lipidated heterodimeric coiled-coil pair E and K it was demonstrated that both peptides have a distinct role in the fusion process and that the peptide-membrane interaction of K is crucial for efficient fusion. Here it's important to note that peptide K is an Amphipathic class A peptide.[40] Amphipathic class A peptides in an α-helical conformation have positive charges adjacent to a hydrophobic surface. This leads to stable membrane immersion of folded helices in phospholipid membranes via an electrostatic interaction between upward bended 'snorkeling' Lys sidechains and phosphate headgroups.[41-42] The peptides designed by Jerala can be regarded as analogs of E and K, but have varying electrostatic charges in positions **e** and **g**, and polar Asn residues in the hydrophobic core resulting in varying degree of class A amphipathicity for individual peptide helices.[43-44] Also, (super)secondary structures and membrane interactions of peptide fusogens are thought to be influential on the fusion efficiency and even the fusogen-membrane distance was found to be crucial for efficient fusion.[40, 45-46] Therefore, using this set of membrane anchored P_E/P_K peptides as fusogens in a liposomal fusion assay the influence of the roleplay of the peptide fusogens on the fusion mechanism and the fusion efficiency will be revealed.

DESIGN OF THE STUDY

Functional membrane tethered complementary recognition motifs as well as soluble N-acetylated peptides were synthesized (*Figure 25*) and the secondary structures of the peptides were measured both in solution and conjugated to phospholipid liposomes. Next, peptide-peptide and peptide-membrane interactions of acylated and lipidated peptides were characterized by temperature and concentration dependent Circular Dichroism (CD) spectroscopy. The ability of the complementary lipidated peptide pairs to mediate fusion was investigated using a content mixing assay. The interactions between the P_E/P_K peptides and the heterodimeric E/K peptide pair were also determined, resulting in the discovery of a new highly fusogenic peptide pair $E/1_K$. Peptide 1_K is the only P-peptide with Lys residues at all **e** and **g** positions, enabling a stable membrane immersion with help of the 'snorkeling' mechanism as was found for peptide K. The interplay of peptide amphipathicity and (super)secondary structures, peptide-membrane interactions and fusogenic efficiency of complementary peptides provides further insight as to the mechanism of peptide mediated fusion of liposomes. Remarkably, very efficient fusion with multiple rounds of fusion was only found for fusogens with moderate stability, showing that significant coiled-coil dissociation after a fusion event is crucial for initiating a next fusion event. This study demonstrates the first step toward orthogonal fusion of peptide functionalized liposomes, revealing a significant and distinct influence of coiled-coil binding strength and peptide-membrane interactions on the fusion efficiency.

PEPTIDE DESIGN AND SYNTHESIS

In this study, 5 heterodimeric coiled-coil peptides and their lipidated derivatives were synthesized. The P_E/P_K four-heptad repeat sequences were taken from Jerala,[34] and the E/K sequences were used previously in membrane fusion studies (Chapter II, *Figure S24*). When folded as helices all peptides possess a small hydrophobic moment. Peptides were synthesized on a Rink Amide resin using automated Solid Phase Peptide Synthesis (SPPS) protocols and Fmoc chemistry. For solution studies the N-termini of the peptides were acylated before cleavage from the resin. For lipopeptide derivatives, the N-termini were functionalized with a PEG spacer of length n (n = 4 or 8 ethylene glycol units) and a

cholesterol anchor.[47] The resulting acylated or lipidated peptides were cleaved from the resin and purified using reverse phase chromatography (RP-HPLC). Details of the peptide design and synthetic protocols are described in the supporting information.

RESULTS AND DISCUSSION

ORTHOGONALITY STUDIES

In the original design by Jerala and coworkers, peptides contained helix-stabilizing N-terminal (SPED) and C-terminal (G) modifications creating flexible, helix-disrupting G-SP tripeptide segments between coiled-coil regions in C-N linked polypeptides. These modifications were omitted in this study because lipidated peptides are used instead of polypeptides. The orthogonality of the coiled-coil pairs and the (super)secondary structure of peptides in solution was studied using CD spectroscopy.[48-49] (*Figure 26, Table 10*) The obtained spectra agree with the orthogonal coiled-coil interactions reported by Jerala, showing that the modifications at the peptide termini did not influence the coiled-coil interactions significantly. All possible peptide-peptide combinations were mixed in an equimolar ratio in PBS to study the orthogonality of this set of 10 coiled-coil peptides.

Table 10. *$\theta_{222}/\theta_{208}$ ratio of all peptide combinations.*

	1_E	1_K	2_E	2_K	3_E	3_K	4_E	4_K	E	K
K	0.64	0.85	0.72	0.39	0.77	0.69	0.66	0.45	1.00	0.63
E	0.42	0.99	0.53	0.43	0.50	0.96	0.62	0.41	0.48	
4_K	0.24	0.34	0.46	0.27	0.41	0.65	1.01	0.32		
4_E	0.39	0.54	0.74	0.47	0.78	0.77	0.71			
3_K	0.41	0.49	0.55	0.63	1.01	0.82				
3_E	0.30	0.76	0.56	0.49	0.62					
2_K	0.25	0.33	1.06	0.34						
2_E	0.38	0.55	0.80							
1_K	1.10	0.39								
1_E	0.20									

Measured $\theta_{222}/\theta_{208}$ ratio of all possible combinations of N-acylated peptides P_E, P_K, E and K. Values >1 are characteristic for coiled-coil formation. [Total peptide] = 200 μM, PBS pH 7.4.

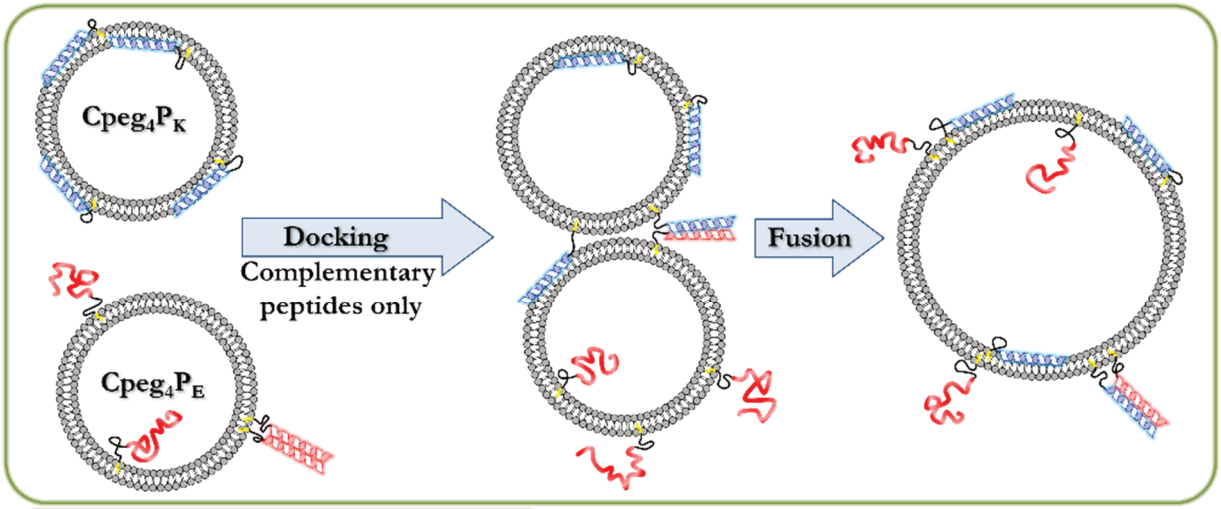

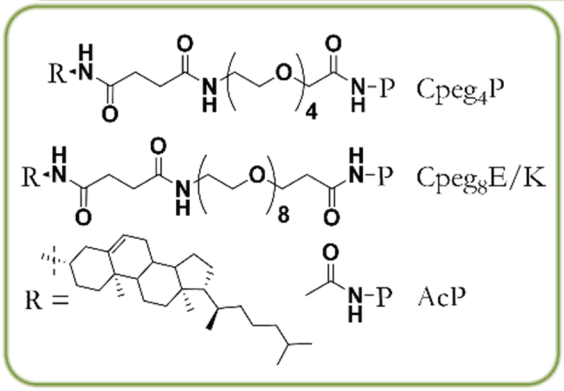

Name (P)	Sequence (gabcdef) [1]
1_E	EIQALEE E**N**AQLEQ E**N**AALEE EIAQLEY
1_K	KIAQLKE K**N**AALKE K**N**QQLKE KIQALKY
2_E	EIQQLEE EIAQLEQ K**N**AALKE K**N**QALKY
2_K	KIAQLKQ KIQALKQ E**N**QQLEE E**N**AALEY
3_E	K**N**AALKE EIQALEE E**N**QALEE KIAQLKY
3_K	E**N**AALEE KIAQLKQ K**N**AALKE EIQALEY
4_E	EIQALEE K**N**AQLKQ EIAALEE K**N**QALKY
4_K	KIAQLKE E**N**QQLEQ KIQALKE E**N**AALEY
E	EIAALEK EIAALEK EIAALEK GY
K	KIAALKE KIAALKE KIAALKE GW

Figure 25. *Schematic overview of orthogonal liposomal recognition and lipopeptide structures. Peptide functionalized liposomes are initially separated, and liposomes dock and fuse due to coiled-coil formation of complementary peptides. The sequences of the used peptides are shown in the table, with highlighted Ile-Asn mutations. The peptide N-terminus was either acetylated or conjugated with the spacer-anchor moieties (Cpeg4 for P-peptides, Cpeg8 for E/K peptides) depicted in the boxed region next to the table.*

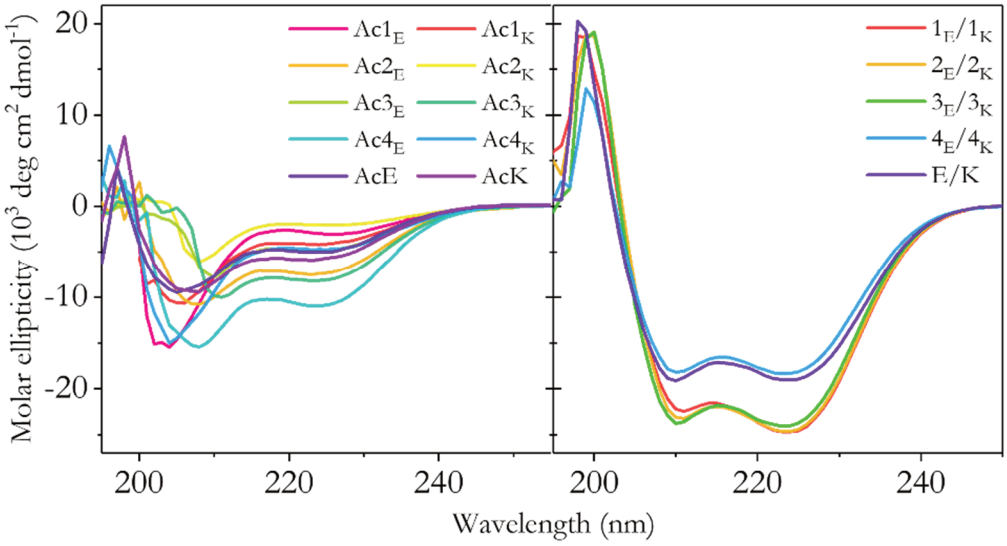

Figure 26. *Left: CD spectra of individual peptides, showing a-helical structures. Right: CD spectra of designed heterodimers, showing typical coiled-coil structures. [Total peptide] = 200 μM, PBS pH 7.4, at 20 °C.*

Intermolecular interaction between different peptides is observed when the θ_{222} value and $\theta_{222}/\theta_{208}$ ratio of the peptide combination has a higher value compared to the averaged value of both single peptides. The CD spectra revealed that peptides do not self-interact significantly and adopt α-helical structures with various degree of helicity. Typical coiled-coil spectra with 2 strong minima at wavelengths of 222 nm and 208 nm and a $\theta_{222}/\theta_{208}$ ratio ≥ 1 were only found for the designed peptide pairs. However, a $\theta_{222}/\theta_{208}$ ratio close to 1 was found for mixtures of E/1_K and E/3_K, indicating a high degree of folding for these hybrid peptide combinations (peptide lengths of 23 and 28 residues respectively). Calculation of their α-helicity values at θ_{222} indicated that only the peptide pair E/1_K formed a significant coiled-coil formation with a relatively high helicity of 42% (*Table S7*). This super secondary structure was rationalized by the helical wheel diagram of the assumed coiled-coil interaction. Coiled-coil formation between P-peptides and E or K is penalized via unfavorable Asn – Ile pairing in the hydrophobic core. However, all **e** and **g** positions of peptide 1_K are occupied by positively charged Lys residues, closely mimicking the charged distribution of peptide K. Since peptide E has Glu residues at complementary **e** and **g** positions, numerous electrostatic interactions are possible. These interactions overcome the polar-apolar Asn – Ile repulsion in the hydrophobic core of a coiled-coil complex.

COILED-COIL BINDING STRENGTH AND OLIGOMER STATE

Next, the binding strength and oligomer state of the found coiled-coil complexes were evaluated using *FitDis!*.[50] This program yields information about oligomeric peptide interactions by fitting both oligomer state and thermodynamics of folding to thermal unfolding curves of the coiled-coil peptide complexes obtained by CD. Thermal unfolding curves were conducted at 25 μM, 50 μM, 100 μM and 200 μM (*Figure 27, Figure S26*). All peptide complexes unfolded between 20 °C and 80 °C but their melting temperatures were lower compared to the values reported by Jerala and coworkers. Therefore, omission of helix stabilizing modifications at peptide termini lowered the strength of the coiled-coil interactions significantly. The strongest interaction at 200 μM was measured in the $1_E/1_K$ peptide pair, with a Tm of 63 °C, while the $4_E/4_K$ pair showed the weakest coiled-coil interaction and unfolded at 37 °C. The other coiled-coil pairs, $2_E/2_K$ and $3_E/3_K$ have a moderate interaction with Tm around 50 °C. For the

interaction of the peptide pair E/1_K a Tm of 30 °C was found. (*Figure 28*) Analysis of the data with *FitDis!* yielded the parameters shown in Table S8. The fitting procedure demonstrated the heterodimeric nature of all coiled-coil peptide pairs, since the root mean square error (RMSE) of the fitted unfolding curves showed a minimum at $\upsilon_1 + \upsilon_2 = 2$ in all cases. Although all used peptides share similar designs and bind in heterodimeric fashion, coiled-coil interactions differ vastly in terms of thermodynamic parameters as quantified with *FitDis!*. (*Table 11*) The peptide pair $1_E/1_K$ shows indeed a strong intramolecular interaction, with a K_F of 5.3×10^7 M^{-1}. Coiled-coil complexes $2_E/2_K$ and $3_E/3_K$ have comparable binding strengths (K_F of ~1.5×10^6 M^{-1}) and are an order of magnitude weaker compared to $1_E/1_K$. The interaction in the coiled-coil complex $4_E/4_K$ is, with a K_F of 2.3×10^5 M^{-1}, two orders of magnitude weaker than $1_E/1_K$ and E/K.

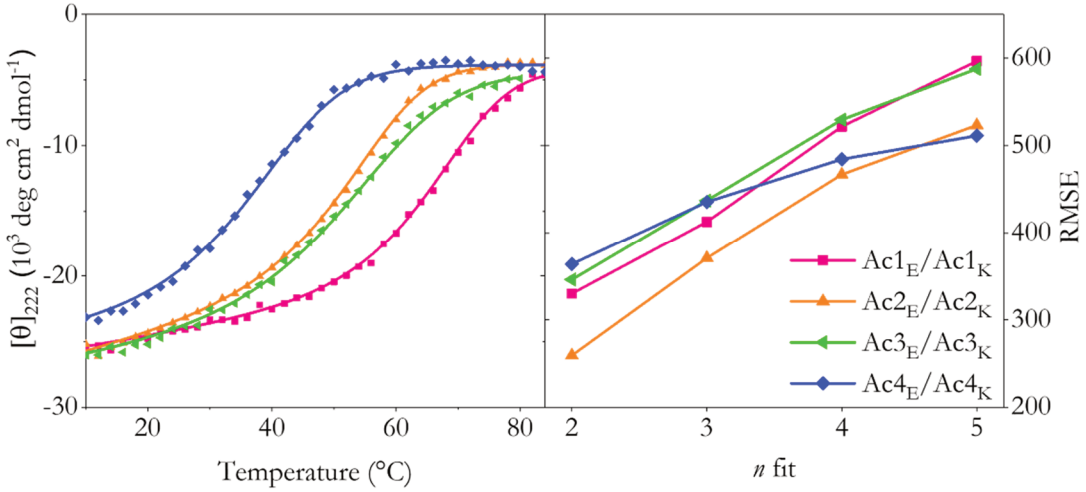

Figure 27. *Thermal unfolding of designed heterodimers $1_E/1_K$ (black), $2_E/2_K$ (red), $3_E/3_K$ (green), and $4_E/4_K$ (blue). Best fits (lines) of experimental data (dots) are obtained using FitDis!. Right graph: RMSE of best fits using different stoichiometric variables shows that the unfolding is best described by a heterodimeric coiled-coil interaction for all peptide sets. [Total peptide] = 200 μM, PBS pH 7.4 at 20 °C.*

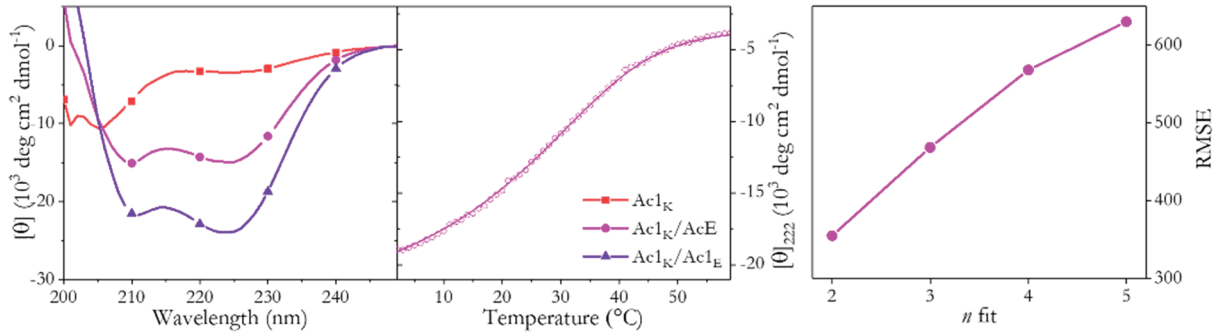

Figure 28. *Analysis of $Ac1_K/AcE$ interaction. Left: characteristic CD spectra of $Ac1_K$, $Ac1_K/AcE$, and $Ac1_K/Ac1_E$ reveal the structural differences between different peptide (super)structures. Middle: thermal unfolding curve of $Ac1_K/AcE$ at 200 μM, and best fit of the experimental data by FitDis!. Right: root mean square error of best fits as a function of stoichiometrics n fit = $\upsilon_1 + \upsilon_2$.*

Table 11. *Thermodynamic parameters at 25°C for P_E/P_K and E/K coiled-coil pairs.*

Coiled-coil	$1_E/1_K$	$2_E/2_K$	$3_E/3_K$	$4_E/4_K$	E/K	$E/1_K$
ΔS_{25} / J mol^{-1} K^{-1}	305	282	248	453	162	291
ΔG_{25} / kJ mol^{-1}	44.1	35.7	34.9	30.6	41.4	24.9
ΔH_{25} / kJ mol^{-1}	135	120	109	166	89.7	112
$K_{F\,25}$ / M^{-1}	5.3×10^7	1.8×10^6	1.3×10^6	2.3×10^5	1.8×10^7	2.3×10^4
$K_{U\,25}$ / M^{-1}	1.9×10^{-8}	5.5×10^{-7}	7.7×10^{-7}	4.4×10^{-6}	5.9×10^{-8}	4.4×10^{-5}

The folding constant of $E/1_K$ is even lower compared to the interactions of the designed coiled-coil pairs with a value of 2.3×10^4 M^{-1}. Comparison of these peptide pairs with E/K shows a similar melting temperature for $1_E/1_K$ and E/K ($K_F = 1.8 \times 10^7$ M^{-1}). Destabilization of the hydrophobic core by two **a**-positional asparagine residues in the $1_E/1_K$ pair is thus balanced by a more stable 4 heptad repeat, compared to the 3 heptad repeat of the E/K peptide pair.

STRUCTURE OF MEMBRANE TETHERED PEPTIDES

To investigate the effect of membrane immobilization on peptide secondary structure, CD spectra were measured for peptide functionalized liposomes, prepared with $Cpeg_4P$ (1-4 mol%), and compared to CD-spectra of solvated peptides. (*Figure S27, Figure S28, Table* S9) Membrane tethered peptides showed an increased helicity compared to N-acetylated peptides; and all peptides adopt partially folded α-helices at 1 mol% decoration except for $Cpeg_41_E$. With increasing [$Cpeg_4P$] at the liposomal membrane, the observed helicity increased, indicative of homo-oligomerization or stabilization of the peptide helix at the membrane surface.[51] Surprisingly, for three lipopeptides β-sheet like structures were found at distinct concentrations: [$Cpeg_42_E$] = 2 mol%, [$Cpeg_42_K$] ≥ 2 mol%, and [$Cpeg_44_K$] ≥ 3 mol% peptide functionalization of the liposomal membrane.

Next, the temperature dependency of the peptides was probed using CD spectroscopy to gain further insight as to the secondary structures and possible membrane interactions of the membrane tethered peptides. Acylated peptides were analyzed in both the absence and presence of liposomes. Secondly, liposomes were decorated with $Cpeg_4$ functionalized lipopeptides and subsequently analyzed, as shown in Figure 29. Because peptide-membrane interactions and homodimer formation of lipopeptides show different concentration dependent unfolding behavior, unfolding curves of $Cpeg_4P$ decorated

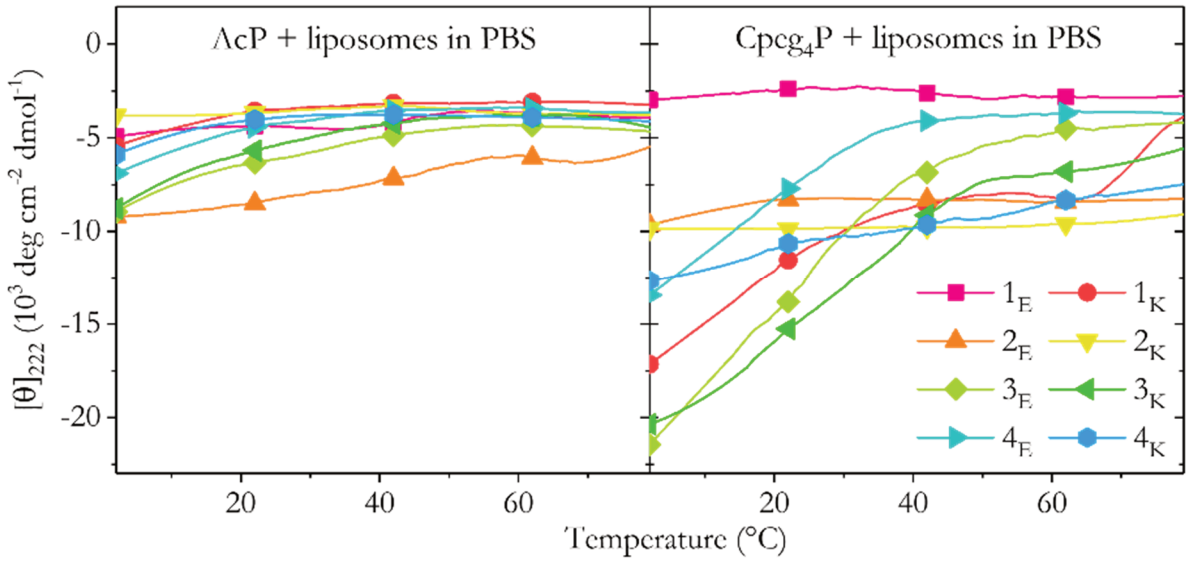

Figure 29. *Left: Temperature dependent unfolding curves of AcP-peptides in the presence of liposomes as determined by θ_{222} absorption. [Total lipid] = 1 mM, [peptide] = 20 μM, in PBS pH 7.4. Right: Temperature dependent unfolding curves of Cpeg4P peptides tethered to liposomes as determined by θ_{222} absorption. [Total lipid] = 0.5 mM, [lipopoptide] = 10 μM (2 mol%), in PBS pH 7.4.*

liposomes were recorded as a function of [Cpeg4P] (2, 3, 4 mol%, Figure S29 - Figure S32). The helical content of N-acetylated peptides, as determined by θ_{222}, did not change significant in the presence of liposomal membranes. In contrast, tethering the peptides to liposomes with Cpeg4 spacers induced structural changes for all derivatives except Cpeg4$1_E$. This shows that Asn incorporation in the hydrophobic core of the P-peptides inhibits a membrane interaction for N-acetylated peptides, since AcK (with a Leu – Ile hydrophobic core) interacts with liposomal membranes. Conversely, the limited degree of freedom of the peg4 spacer forces all peptides (except 1_E) in distinct secondary structures, but differences in supramolecular interactions were observed between the different lipopeptides. The thermal unfolding curves suggest that Cpeg4$1_K$ and Cpeg4$3_K$ have interactions with their membranes according to the increased helicity still occurring at 60 °C, but homodimer formation is also possible.[51] Interestingly, peptide 1_K is the only P-peptide with Lys residues at all **e** and **g** positions, which could enable a stable membrane immersion with help of the 'snorkeling' mechanism as was found for peptide K.[40] Cpeg4$3_E$ and Cpeg4$4_E$ show increased helicities at room temperature but similar helicities at 60 °C compared to their N-acetylated derivatives, indicative of homodimer formation. Conversely, the melting curves of membrane tethered Cpeg4$2_E$, -2_K and -4_K support the observed β-sheet formation with an increased θ_{222} and a low or absent temperature dependency.

LIPOSOME DOCKING

Docking of liposomes is facilitated via coiled-coil formation between complementary peptides tethered to liposomes. The change in peptide structure was measured using CD spectroscopy; liposomes functionalized with complementary peptides were mixed and the resulting CD spectra before and after mixing are shown in Figure 30 and Table 12.

Significant differences in coiled-coil binding between all above described coiled-coil peptide pairs was observed upon mixing of peptide functionalized liposomes. The increase in %H and a $\theta_{222}/\theta_{208}$ closer to 1 indicates coiled-coil formation for mixtures of liposomes decorated with lipopeptide fusogens $2_E/2_K$, $3_E/3_K$, E/K and $E/1_K$ with respect to the obtained values of liposomes prior to mixing. In contrast, the observed low values for %H and $\theta_{222}/\theta_{208}$ for mixtures of liposomes decorated with lipopeptides $1_E/1_K$ and $4_E/4_K$ are illustrative for the absence of coiled-coil superstructures.

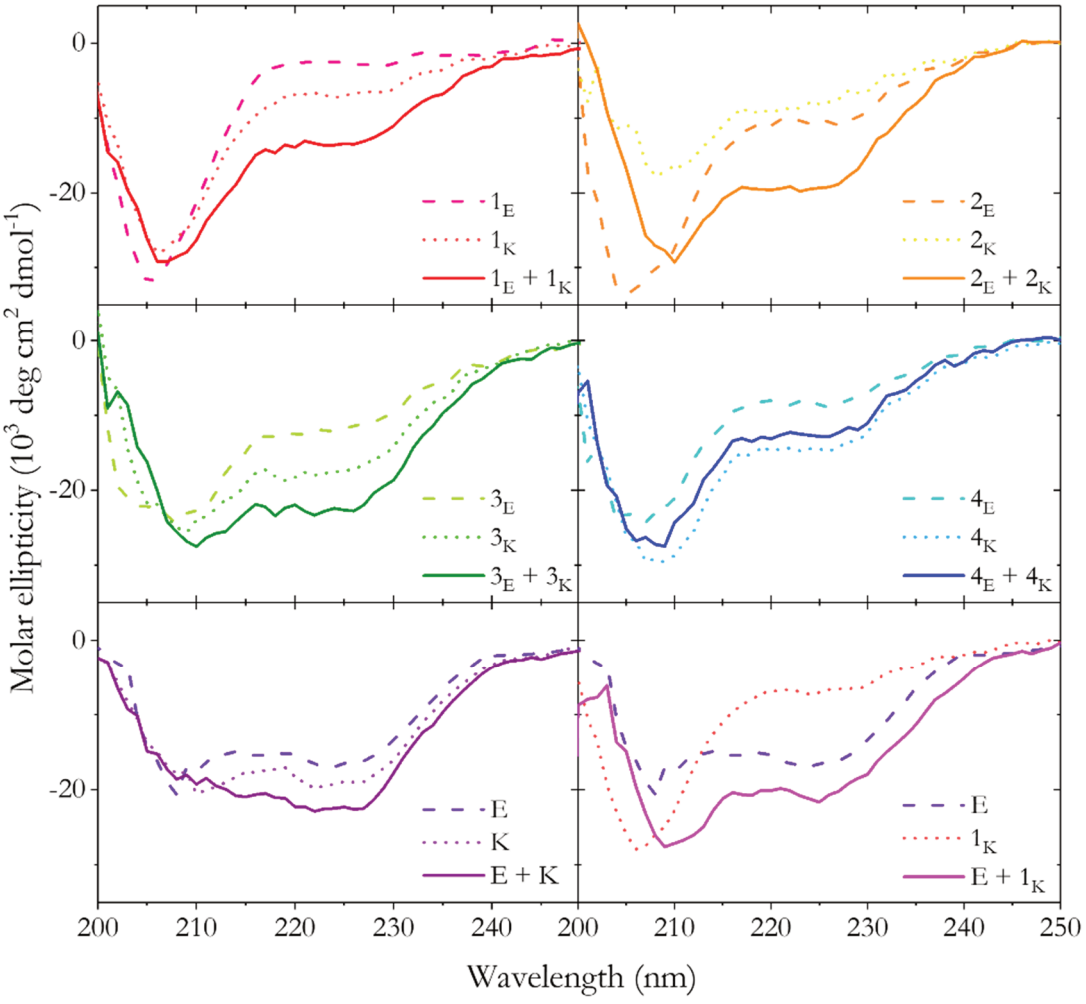

Figure 30. *CD spectra of liposomes decorated with $Cpeg_4P$ or $Cpeg_8E/K$, and the equimolar mixture of liposomes bearing complementary peptides. [Total lipid] = 0.5 mM, with 1 %mol lipopeptide, PBS pH 7.4, 20 °C.*

Table 12. *Degree of peptide helicity before and after mixing of peptide functionalized liposomes.*

Peptide		1_E	1_K	2_E	2_K	3_E	3_K	4_E	4_K	E	K	1_K	E
$Cpeg_4$	%H	8	20	30	26	36	53	25	44	52	60	20	52
	$\theta_{222}/\theta_{208}$	0,1	0,2	0,3	0,5	0,5	0,7	0,4	0,5	0,9	1,0	0,2	0,9
$Cpeg_4P_E$+ $Cpeg_4P_K$	%H	40		58		69		37		71		61	
	$\theta_{222}/\theta_{208}$	0,5		0,7		0,9		0,5		1,2		0,8	

[Lipopeptide] = 5 μM, and [total lipid] = 0.5 mM. Recorded in PBS pH 7.4, 20 °C.

CONTENT MIXING ASSAY

Content mixing in the absence of leakage is regarded as a completed fusion event between two liposomes. We use a quantitative content mixing model for populations of small liposomes by encapsulating the water-soluble dye Sulphorhodamine B.[47, 52-53] The dye is self-quenched at high concentrations, which upon dilution results in relief of self-quenching and concomitant fluorescence increase. In these experiments $Cpeg_4$ functionalized P-peptides and $Cpeg_8$ functionalized E/K peptides were used to account for the shorter peptide length of E/K compared to P-peptides; also, $Cpeg_8E/K$ is more fusogenic than $Cpeg_4E/K$.[46] Therefore, one batch of liposomes bearing peptide $Cpeg_4P$ was loaded with 20mM sulphorhodamine B in PBS, and mixed with peptide $Cpeg_4P$-, $Cpeg_8E$- or $Cpeg_8K$-functionalized buffer-containing liposomes. The fluorescence increase was followed for 30 minutes. (*Figure 31, Figure S33*)

Fluorescence increase was only observed with a few coiled-coil pairs: Efficient fusion of liposomes (>40% content mixing) was obtained when cholesterol anchored $2_E/2_K$, $3_E/3_K$ or $E/1_K$ were used as fusogens. Liposomes functionalized with cholesterol anchored $1_E/1_K$ or combinations of lipopeptides P and K yielded only <25% content mixing. The $Cpeg_41_K/Cpeg_8E$ peptide pair was even more efficient in mediating fusion than the designed $Cpeg_8E/Cpeg_8K$ fusogen (±50% content mixing), which again demonstrated the influence of both peptides on the efficiency of the fusion process. Conversely, liposome fusion was not initiated by the complementary peptides $Cpeg_44_E/Cpeg_44_K$ and by all other non-complementary peptide combinations. It is evident that fusion only occurs when coiled-coil formation is established between complementary peptides tethered to opposing liposomes. The absence of fusion for

liposomes functionalized with $Cpeg_4 4_E$/$Cpeg_4 4_K$ agrees with the absence of coiled-coil formation observed for liposomes functionalized with these peptides. The high selectivity of the orthogonal fusion system is further illustrated by the absence of fusion when non-complementary $Cpeg_4P$ peptides are used. On the other hand, fusion efficiencies of ±20% were found with almost all liposomal mixtures involving $Cpeg_8K$ decorated liposomes, demonstrating the high fusion activity of the amphipathic K peptide.

STRUCTURE-ACTIVITY RELATIONSHIP OF FUSOGENS

Analysis of the peptide structure could shed light on the required peptide characteristics for fusion. As shown in Figure 32, some correlation is found between CC binding strength, helicity of the peptide structures and fusion efficiency. Efficient fusogens are characterized by relatively high peptide helicities and low fusion efficiencies are accompanied with relatively low helicities of the involved fusogens.

Comparison of the fusogens $1_E/1_K$, $2_E/2_K$, $3_E/3_K$, $4_E/4_K$ and E/K showed that peptides with higher helicities before fusion reach higher fusion efficiencies, suggesting that fusion is enhanced by pre-formed helices. But we also hypothesized previously that CpegE/CpegK peptide mediated liposome fusion is mainly driven by the characteristic membrane destabilization of peptide CpegK.[40] For the $Cpeg_4P$ peptides, CD measurements suggest peptide-membrane interactions for only 1_K and 3_K, which correlates very well with the high fusion efficiency of $Cpeg_4 1_K$/$Cpeg_8E$ and $Cpeg_4 3_E$/$Cpeg_4 3_K$, supporting this hypothesis. The importance of a peptide-membrane interaction in agreement with SNARE-mediated membrane fusion, in which the proteins not only bring opposing membranes in close proximity, but also play an active role in overcoming subsequent fusion barriers by applying mechanical stress to the membranes of fusion intermediates.[54-55] Also, 1_K and 3_K are the only P-peptides having lysine residues occupying positions **e** and **g** of the 2nd and 3th heptad, indicating some correlation between positive charges at these positions and a higher fusogenic activity and/or a more profound membrane interaction. Interestingly, the membrane-interacting fusogens $E/1_K$, $3_E/3_K$ and E/K exhibit a reverse relationship between fusion efficiency and CC binding strength, whereas lipopeptides $1_E/1_K$, $2_E/2_K$ and $4_E/4_K$ show no apparent influence of the CC binding strength of the fusion efficiency. Therefore, binding strength of the fusogens is not the main driving force of coiled-coil peptide mediated fusion, as was

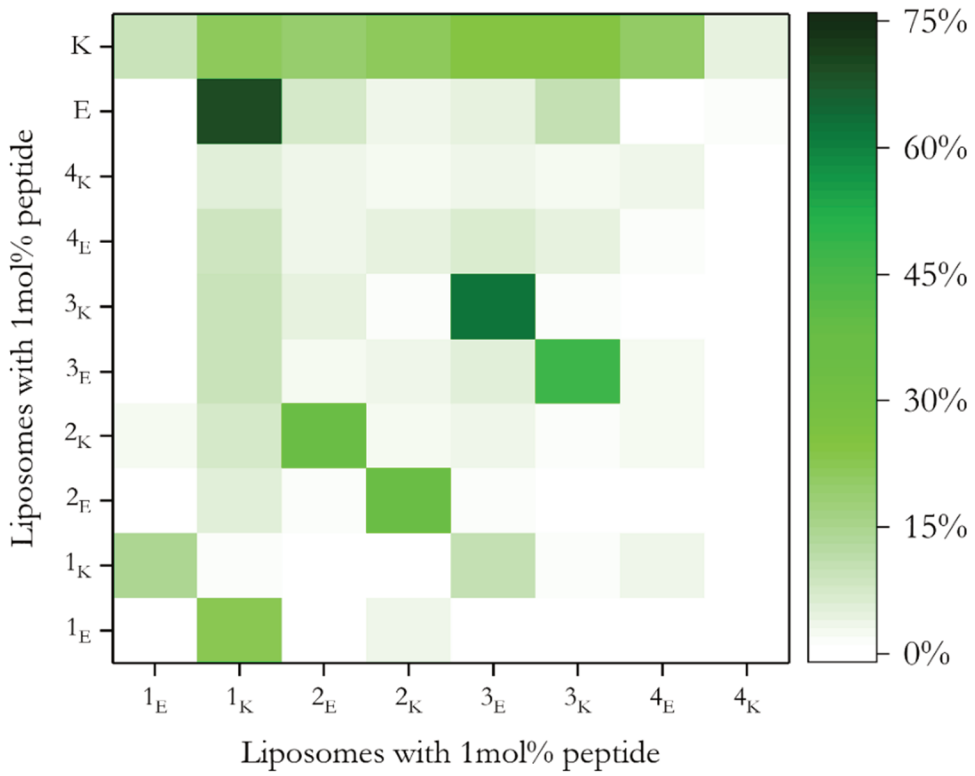

Figure 31. *Membrane fusion assay. Content mixing between vesicles loaded with Sulphorhodamine B (x-axis) and plain vesicles (y-axis), as a function of peptide derivative, after 30 minutes. [Total lipid] = 0.1 mM, with 1mol% lipopeptide in PBS pH 7.4 at 20 °C.*

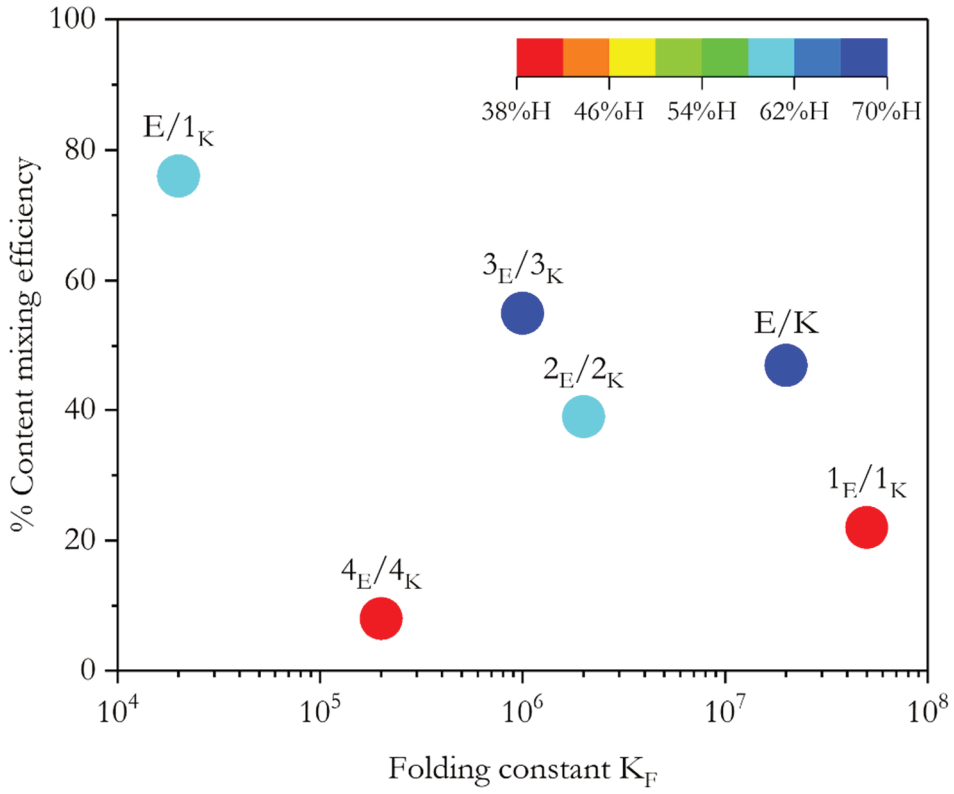

Figure 32. *Content mixing efficiency as a function of KF of the heteromeric peptide pair. Colors correspond to helicities of peptide functionalized liposomes.*

hypothesized for other fusion model systems.[21] Fusogens used in those model systems do not interact with liposomal membranes, and solely facilitate docking of liposomes. The very close apposition of both liposomes itself causes the fusion process to proceed, without further influence of the fusogen.

Here, a similar behavior was observed for the fusogen $2_E/2_K$.Both lipopeptides do not interact with their supportive membranes, as shown with CD measurements, and are most likely only facilitating liposomal docking. The obtained moderate fusion efficiency with this fusogen (40%) further supports our hypothesis that fusogen-membrane interactions are crucial for efficient fusion.

Comparison of the $Cpeg_41_K/Cpeg_41_E$ and $Cpeg_41_K/Cpeg_8E$ fusogens reveal the remarkable influence of the counter-peptide on the efficiency of the fusion process. $Cpeg_41_E$ and $Cpeg_8E$ are both negatively charged peptides, but their secondary structures differ vastly. CD spectra of $Cpeg_41_E$ indicate a random coil conformation, while $Cpeg_8E$ was found to be mainly in a homodimeric coiled-coil conformation at room temperature. Also, peptide helicity increased to 61% upon mixing of $Cpeg_41_K$ and $Cpeg_8E$ functionalized liposomes while a mixture of $Cpeg_41_K/Cpeg_41_E$ functionalized liposomes only showed 40% helicity although the binding strength of $Ac1_K/Ac1_E$ is 3 orders of magnitude larger compared to Ac1K/AcE.

The higher local peptide concentration and the highly ordered structure of $Cpeg_8E$ over $Cpeg_41_E$ could enhance the peptide availability to bind with $Cpeg_41_K$, as indicated by the relatively high helicity of $Cpeg_41_K/Cpeg_8E$, thereby enhancing the fusion efficiency. Secondly, visible aggregates of liposomes were only observed when $Cpeg_41_K/Cpeg_8E$ were used as fusogens, as was found for $Cpeg_{12}E$/ $Cpeg_{12}K$ fusogens also.[46] However, aggregation of liposomes was not observed when $Cpeg_42_E/Cpeg_42_K$ and $Cpeg_43_E/Cpeg_43_K$ were used as fusogens. These observations suggest that formation of micron sized assemblies is due to the occurrence of multiple rounds of fusion, because the affinity of $Cpeg_41_K/Cpeg_8E$ is too low to trigger aggregation of liposomes specifically. Furthermore, multiple rounds of fusion are only possible when a considerable amount of the involved fusogens disassociate after the fusion process, which is enhanced by the low binding strength of $Cpeg_41_K/Cpeg_8E$. Therefore, the high fusion efficiency of this specific peptide pair is likely due to the combination of the enhanced availability of the

homodimer $Cpeg_8E$, the presumable membrane interaction of $Cpeg_41_K$ and the very transient heterodimeric coiled-coil interaction.

CONCLUSIONS

This study demonstrated the orthogonal interactions of a library of lipidated coiled-coil peptides. The interactions of these peptides with the coiled-coil peptide pair E/K were investigated also, and a minor interaction was found between 1_K and E. Coiled-coil stability and oligomeric state were determined with concentration and temperature dependent CD spectroscopy. Also, the observed secondary structure of almost all $Cpeg_4P$ peptides was affected by membrane tethering due to increased local concentration.

It was shown that various coiled-coil peptides can mediate membrane fusion, and efficient orthogonal content mixing was obtained between liposomes decorated with the lipopeptide pairs $2_E/2_K$, $3_E/3_K$, and $E/1_K$. Examination of peptide structure and fusogenic efficiency revealed that transient coiled-coil interactions enhance the fusion process. Furthermore, fusogens with clear asymmetric roles were found to be highly fusogenic. Two roles could be identified: An active role with a membrane interacting peptide, and a passive role with a highly accessible peptide homodimer. This active – passive roleplay was found for the efficient fusogens $3_K/3_E$ and $E/1_K$ (and the well described E/K pair), respectively. The fusogen $2_E/2_K$ lacked this distinct roleplay and mediated fusion by forcing liposomes just in close proximity, thereby reaching only moderate fusion efficiencies.

The high efficiency of the $Cpeg_41_K/Cpeg_8E$ fusogen makes these peptides useful candidates for liposome – cell fusion assays.[47, 56-57] Other favorable characteristics of this fusogen are the very transient coiled-coil interaction which increases peptide availability after a successful fusion event and the absence of nonspecific fusion events. Above all, this research lays the foundations for the development of partner specific liposome – cell fusion models and supramolecular self-assembly of peptide functionalized building blocks.

EXPERIMENTAL SECTION

MATERIALS

Fmoc-protected amino acids, rink amide resin, and O-(1H-6-Chlorobenzotriazole-1-yl)-1,1,3,3-tetramethyluronium hexafluorophosphate (HCTU) were purchased from NovaBioChem. Diisopropylethylamine (DIPEA), piperidine, acetic anhydride, N-methylpyrrolidine (NMP), dimethylformamide (DMF), acetonitrile, and trifluoroacetic acid (TFA) were obtained from Biosolve. Dichloromethane (DCM), diethyl ether, triisopropylsilane (TIS), trimethylamine (TEA), trifluoroethanol (TFE), cholesterol, trimethylphosphine (1M in toluene), (1H-benzotriazol-1-yloxy) tripyrrolidinophosphonium hexafluorophosphate (PyBOP), succinic anhydride, and sulforhodamine B were obtained from Sigma Aldrich. 1,2-dioleoyl-sn-glycero-3-phosphatidylcholine (DOPC), and 1,2-dioleoyl-sn-glycero-3-phosphatidylethanolamine (DOPE) were purchased from Avanti polar lipids. The N_3–$(PEG)_4$–COOH spacer[58-59] and Cholesteryl-4-amino-4-oxobutanoic acid[60] were synthesized according to literature procedures. PBS buffer contains 5 mM KH_2PO_4, 15 mM K_2HPO_4, 150 mM NaCl, pH 7.4. Data analysis and visualization was performed using OriginPro 9.1.

METHODS

Liposome preparation. A 1 mM stock solution containing DOPC/DOPE/cholesterol (50:25:25 mol%) in 1:1 (v/v) chloroform/methanol was prepared for all fusion experiments. Lipopeptides (50 μM) were dissolved in 1:1 (v/v) chloroform/methanol. In general, 1 mol% of the lipopeptide solution was mixed with the liposome solution and the solvent was removed under a stream of N_2. One lipid/lipopeptide film was rehydrated with PBS (1 mL). A second lipid/lipopeptide film was rehydrated with PBS buffer containing 20 mM sulforhodamine B (1 mL). The solutions were briefly vortexed and subsequently sonicated for 5-10 minutes at 55 °C to yield ~100 nm diameter liposomes, verified with dynamic light scattering (DLS).[61] Solutions of plain liposomes were used without further purification, whereas sulforhodamine B containing liposomes were purified using a Sephadex G25 column to remove any non-encapsulated sulphorhodamine B. The purification dilution factor was 1:5.

Fluorescence spectroscopy. Content-mixing experiments were performed on a TECAN Infinite M1000 PRO fluorimeter using a 96-well plate at 25 °C. The percentage of fluorescence increase, *%F*, was calculated as

$$\%F = \frac{F(t) - F_0}{F_{max} - F_0} * 100$$

Content mixing experiments: The sulphorhodamine B fluorescence intensity, *F(t)*, at 580 nm was monitored in a continuous fashion for 30 min after mixing non-fluorescent liposomes with sulphorhodamine B loaded liposomes. F_0 was obtained by measuring the emission of sulphorhodamine B-loaded liposomes to which an equal amount of PBS was added, and F_{max} was obtained by measuring the emission of plain liposomes loaded with 10 mM sulphorhodamine B. [Total lipid] = 0.1mM, in PBS pH 7.4, 25 °C.

Dynamic Light Scattering. Particle size distributions were measured by dynamic light scattering using a Malvern Zetasizer Nano ZS ZEN3500 equipped with a peltier thermostatic cell holder. The laser wavelength was 633nm and the scattering angle was 173°. The Stokes Einstein relationship

$$D = \frac{k_B T}{3\pi\eta D_h}$$

was used to estimate the hydrodynamic diameter D_h. Here, k_B is the Boltzmann constant, η is the solvent viscosity, and measurements were carried out at room temperature. For size increase experiments, 0.5mM liposomes functionalized with 1 mol% lipopeptide were prepared. Upon mixing of lipopeptide bearing liposomes, size distribution was followed for 30 min.

Circular Dichroism Spectroscopy. CD spectra were obtained using a Jasco J-815 spectropolarimeter equipped with a peltier temperature controller. The ellipticity, given as mean residue molar ellipticity, [θ] (deg cm^2 dmol^{-1}), is calculated using the following equation

$$[\theta] = \frac{100 * \theta_{obs}}{nlc}$$

where θ_{obs} is the observed ellipticity (mdeg), *n* is the number of peptide residues, *l* is the path length of the cuvette (cm) and *c* is the peptide concentration (mM). Spectra were recorded from 260 nm to 200 nm at 20 °C. Data points were collected with a 1 nm bandwidth at 1 nm intervals, using a scan speed of 1 nm s-1. Each spectrum was an average of five scans. For analysis, each spectrum had the background spectrum (plain liposomes in PBS) subtracted. The percentage α-helicity was calculated using the predicted value $[\theta]_{222}$ = -39500*(1-2.57/n) as 100% value for an α-helical peptide of n residues.[62] For temperature dependent measurements $[\theta]_{222}$ was recorded as a function of temperature, with a range of 2 - 80°C and ΔT = 40°C/h. Cuvette path length = 2mm, [total lipid] = 0.5 or 1mM, with 1, 2, 3 or 4 mol% lipopeptide, in PBS at pH 7.4.

PEPTIDE SYNTHESIS

Peptide Synthesis: Peptide synthesis was performed on a CEM Liberty I peptide synthesizer on a 100 μM scale using Rink amide resin (0.55-0.73 mmol/g). Amino acid activation was achieved using HCTU/DIPEA (4eq/6eq) in DMF. Fmoc-deprotection was carried out using two cycles of 20% piperidine in DMF. All reactions were carried out at 70-80 °C using microwave irradiation for three minutes.

Acylated peptides: The N-terminal free amine was acylated using a mixture of Ac_2O (50 mM) and DIPEA (12.5 mM) in NMP for 1h. The resin was washed thoroughly with DMF and DCM to remove excess reactants.

Lipopeptides: The N_3-Peg_4-COOH spacer was conjugated to the peptide free N-terminus using PyBOP/DIPEA activation (3eq/5eq) in DMF containing LiCl (1mg/mL) for 2h. N_3-PEG_4-COOH-containing peptides were reduced using two cycles of PME in dioxane/water (4:1). Cholesteryl-4-amino-4-oxobutanoic acid was activated with PyBOP/DIPEA (3eq/5eq) in DCM/DMF 1:1, added to the resin-bound peptides and the reaction was shaked for two days at rt. The resin was washed thoroughly with DMF and DCM to remove excess reactants.

Cleavage: The (lipo)peptides were cleaved from the resin and side-chain deprotected using a mixture of TFA/TIS/H_2O (95:2.5:2.5 v/v) for 2h. The (lipo)peptides were precipitated in cold diethyl ether followed by centrifugation and dried under vacuum.

Purification: RP-HPLC was performed with a Shimadzu HPLC system with two LC-8A pumps, and a SPD-10AVP UV-VIS detector. Sample elution was monitored by UV detection at 214 nm and 278 nm. Samples were eluted with a linear gradient from 10% to 90% (v/v) B in A, A being H_2O, 0.1% (v/v) TFA, and B being MeCN, 0.1% (v/v) TFA. Purification of (lipo)peptides was performed on a Phenomenex C18 reversed phase column (21.2 mm diameter, 150 mm length, 5.00 μM particle size) with a flow rate of 15 mL min^{-1}. Collected fractions were tested for >95% purity using LC-MS with Gemini C18 column and freeze dried.

PEPTIDE SEQUENCES AND HELICAL WHEEL OF P-PEPTIDES

Asn-Asn (N) and Ile-Ile (I) are both inserted twice in the hydrophobic core of each coiled-coil pair at position **a**, with different positions for the individual orthogonal pairs and thereby enhancing pairing specificity. For electrostatic interactions at positions **e** and **g**, Glu (E) and Lys (K) were used as charged residues,[63] with opposite charges at complementary heptads within the paired heterodimer. Again, the electrostatic pattern along the coiled-coil complex differs for all orthogonal pairs, contributing to partner specificity. E $(EIAALEK)_3$ and K $(KIAALKE)_3$ are also shown for comparison.

Table S4. *The used sequences of peptides P_E / P_K, and E / K.*

Name	Sequence $(gabcdef)_4$ [1]	Hydrophobic pattern [2]	Electrostatic pattern [2]
1_E	EIQALEE ENAQLEQ ENAALEE EIAQLEY	I N N I	E E E E
1_K	KIAQLKE KNAALKE KNQQLKE KIQALKY	I N N I	K K K K
2_E	EIQQLEE EIAQLEQ KNAALKE KNQALKY	I I N N	E E K K
2_K	KIAQLKQ KIQALKQ ENQQLEE ENAALEY	I I N N	K K E E
3_E	KNAALKE EIQALEE ENQALEE KIAQLKY	N I N I	K E E K
3_K	ENAALEE KIAQLKQ KNAALKE EIQALEY	N I N I	E K K E
4_E	EIQALEE KNAQLKQ EIAALEE KNQALKY	I N I N	E K E K
4_K	KIAQLKE ENQQLEQ KIQALKE ENAALEY	I N I N	K E K E
E	EIAALEK EIAALEK EIAALEK GY	I I I	E E E
K	KIAALKE KIAALKE KIAALKE GW	I I I	K K K

[1] All peptides contain a N-terminal acyl and C-terminal amide. [2] The designed orthogonal interactions are illustrated by differences in hydrophobic (position a) and electrostatic patterns (positions e and g) between the peptide pairs.

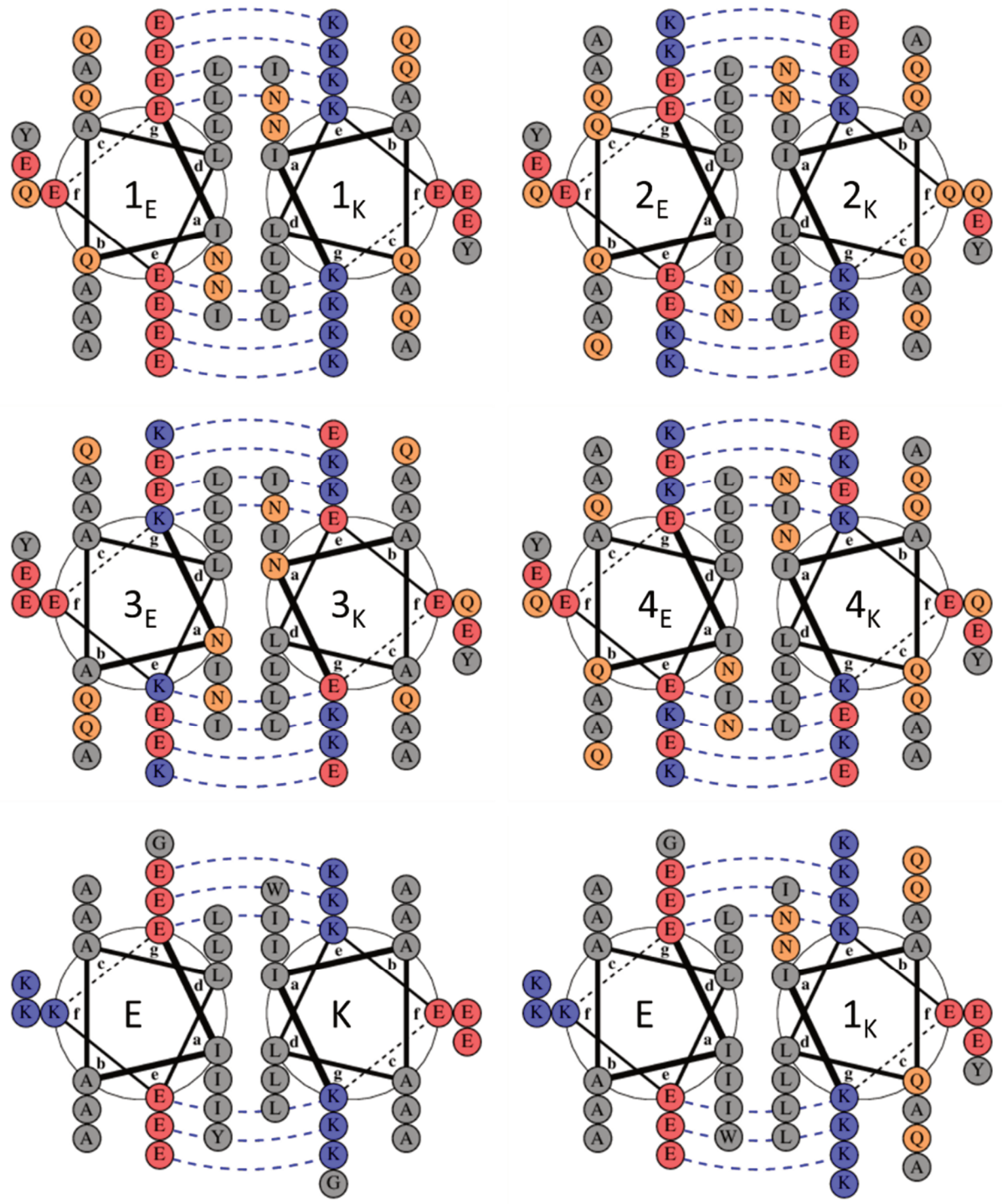

Figure S24. *Helical wheel projection of the coiled-coil pairs, illustrating the designed electrostatic and hydrophobic interactions stabilizing the coiled-coil formation. Helical wheels were made using Drawcoil 1.0.*

PEPTIDE ANALYSIS

Peptide purity was confirmed using LC-MS analysis equipped with Gemini 3µ C18 column coupled with Finningan LCQ advantage max (Thermo) ESI-MS analyzer and the results are summarized in Table S5. LCMS eluents were A) H2O + 0.1% v/v TFA, B) MeCN + 0.1% v/v TFA, with a flow rate of 1 mL min^{-1}. Gradient for acylated peptides was applied from 2 to 30 min, from 10% B in A to 90% B in A, while the same gradient was applied for lipopeptides from 1 to 12 min. Retention time RT is rounded to 2 significant numbers.

Table S5. *Analysis of AcP Peptides*

Peptide	Formula	Calc. mass	Observed mass	RT (min)	Isoelectric point[a]	Charge[a]
$Ac1_E$	$C_{140}H_{219}N_{35}O_{56}$	3288.458	3312.325 $[M+Na]^+$	22	2.78	-10.0
$Ac1_K$	$C_{150}H_{261}N_{43}O_{42}$	3338.963	3340.463 $[M+H]^+$	12	10.40	+4.8
$Ac2_E$	$C_{146}H_{242}N_{40}O_{49}$	3341.744	3343.847 $[M+H]^+$	19	4.62	-2.1
$Ac2_K$	$C_{146}H_{243}N_{41}O_{48}$	3340.759	3342.646 $[M+H]^+$	16	4.92	-1.1
$Ac3_E$	$C_{144}H_{238}N_{38}O_{49}$	3285.677	3287.231 $[M+H]^+$	20	4.44	-3.1
$Ac3_K$	$C_{142}H_{236}N_{38}O_{47}$	3227.641	3229.010 $[M+H]^+$	18	4.62	-2.1
$Ac4_E$	$C_{144}H_{239}N_{39}O_{48}$	3284.692	3287.046 $[M+H]^+$	17	4.62	-2.1
$Ac4_K$	$C_{146}H_{242}N_{40}O_{49}$	3341.744	3344.621 $[M+H]^+$	16	4.62	-2.1

[a] *Calculated with Isoelectric Point Calculator and peptide charge is calculated at pH 7.4.*[64]

Table S6. *Analysis of synthesized lipopeptides*

Peptide	Formula	Calc mass	Observed mass	RT (min)
$Cpeg41_E$	$C_{179}H_{284}N_{36}O_{63}$	3948.36	1974.80 $[M+2H]^{2+}$	11
$Cpeg41_K$	$C_{189}H_{326}N_{44}O_{49}$	3998.86	1357.73 $[M+3Na]^{3+}$	7.4
$Cpeg42_E$	$C_{185}H_{307}N_{41}O_{56}$	4001.65	1335.00 $[M+3H]^{3+}$	9.2
$Cpeg42_K$	$C_{185}H_{308}N_{42}O_{55}$	4000.66	1334.60 $[M+3H]^{3+}$	8.6
$Cpeg43_E$	$C_{183}H_{303}N_{39}O_{56}$	3945.58	1973.47 $[M+2H]^{2+}$	8.7
$Cpeg43_K$	$C_{181}H_{301}N_{39}O_{54}$	3887.54	1944.27 $[M+2H]^{2+}$	9.0
$Cpeg44_E$	$C_{183}H_{304}N_{40}O_{55}$	3944.59	1973.53 $[M+2H]^{2+}$	9.6
$Cpeg44_K$	$C_{185}H_{307}N_{41}O_{56}$	4001.65	1334.93 $[M+3H]^{3+}$	9.3

CD SPECTRA OF PEPTIDE-PEPTIDE INTERACTION

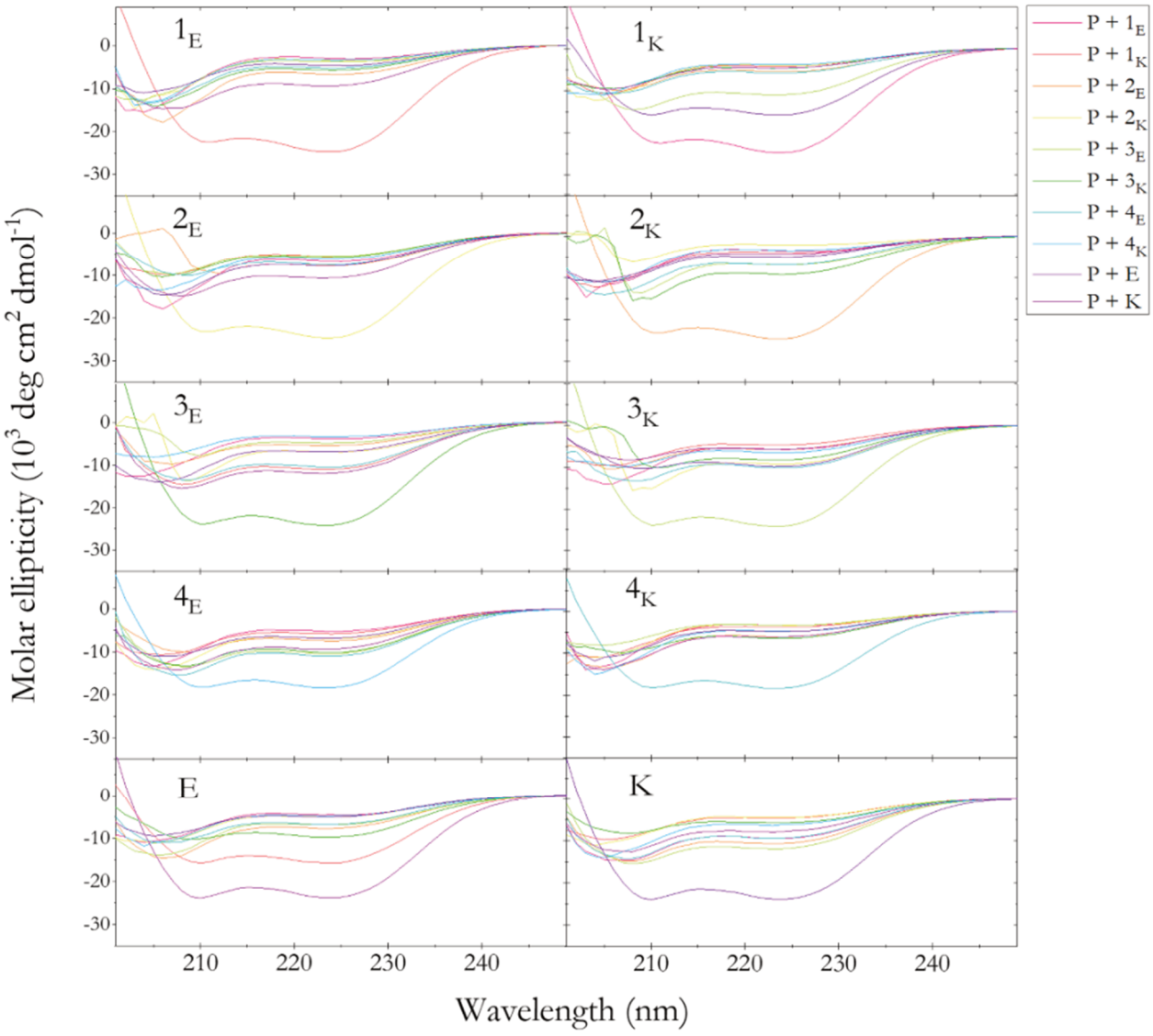

Figure S25. *CD spectra of P-peptide combinations. [Total peptide] = 200 μM, in PBS pH 7.4*

Table S7. *Helicity of equimolar peptide combinations*

Peptide	1_E	1_K	2_E	2_K	3_E	3_K	4_E	4_K	E	K
K	24	10	27	10	31	14	24	15	52	15
E	11	42	19	12	17	25	17	11	9	
4_K	7	9	15	8	8	16	49	11		
4_E	13	14	19	17	27	26	29			
3_K	14	11	11	19	65	22				
3_E	9	29	10	14	13					
2_K	8	9	67	5						
2_E	17	13	21							
1_K	67	10								
1_E	7									

Percentage α-helicity was calculated using the formula $[\theta]_{222} = -39500*(1-2.57/n)$ to obtain a 100% helicity value for an α-helical peptide of n residues.[62] For E/K, n = 23; For $P_{E/K}$, n = 28; For mixtures of E/K and P-peptides, n = 25.5. [Total peptide] = 200 μM, PBS pH 7.4 at 20 °C.

CONCENTRATION DEPENDENT THERMAL UNFOLDING CURVES

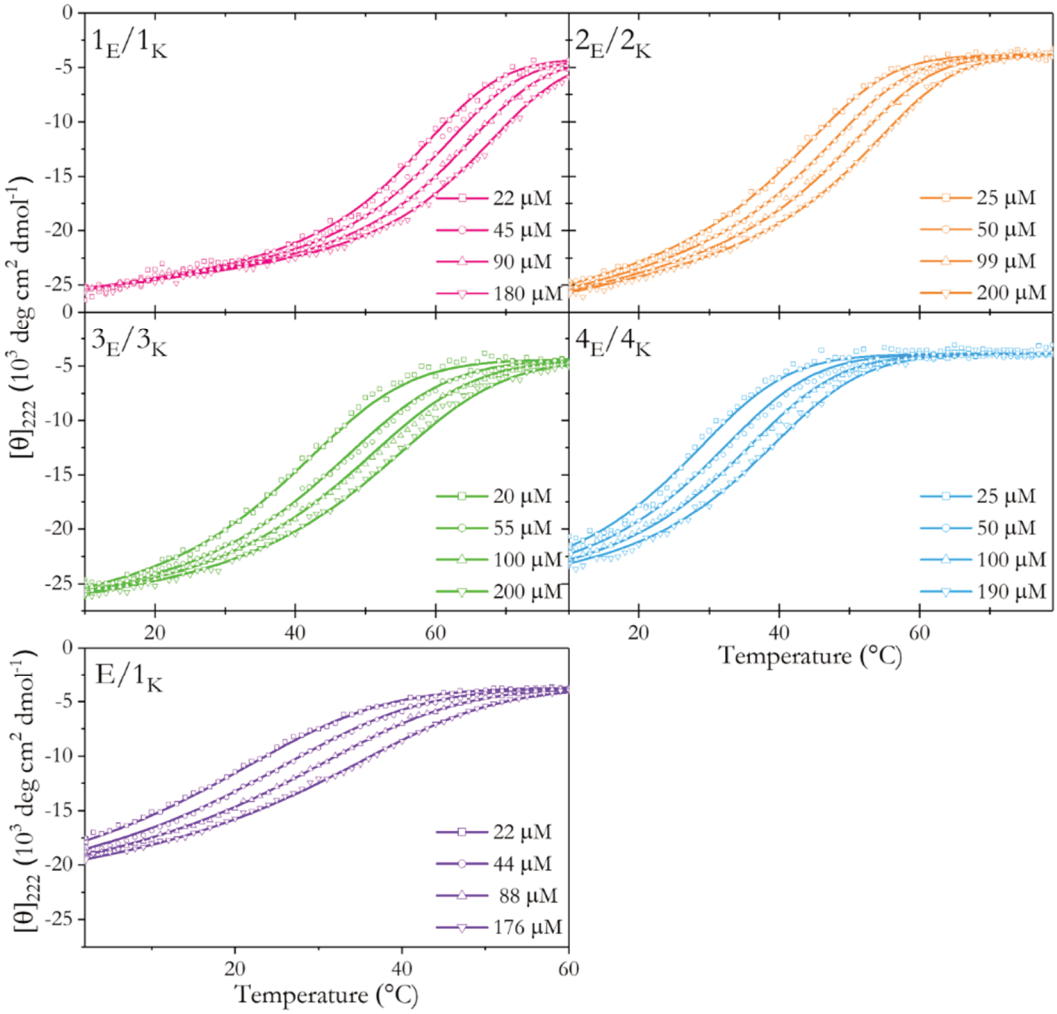

Figure S26. *Concentration dependent thermal unfolding of designed heterodimers $1_E/1_K$, $2_E/2_K$, $3_E/3_K$, $4_E/4_K$ and $E/1_K$. Best fits (lines) of experimental data (dots) are obtained using FitDis!.[50] In PBS, pH 7.4.*

Table S8. *Parameters for formal description of P-peptide complexes and the E-K complex.*

Coiled-coil	$1_E/1_K$	$2_E/2_K$	$3_E/3_K$	$4_E/4_K$	E/K [c]	$E/1_K$
$P_{Tmin} - P_{Tmax}$ / μM [a]	22 – 180	25 – 200	20 – 200	25 – 190	3 – 25	44 – 380
Found υ_1, υ_2, υ_3,. [b]	1,1	1,1	1,1	1,1	1,1	1,1
Tm / °C (200 μM)	63	50	51	37	67	32
ΔH° / kJ mol^{-1} [d]	282	281	171	194	215	163
T° / °C [d]	107	92	114	88	144	92
ΔC_P / kJ mol^{-1} K^{-1} [d]	1.6	2.5	0.3	0.8	1.1	0.8
θ_{F0} / 10^3	-26.2	-27.3	-27.0	-24.7	-29.9	-20.7
m_{F0}	78.2	113.4	84.8	60.4	94.5	76.4
θ_{U0} / 10^3	-4.1	-3.8	-4.4	-3.9	-5.8	-3.7
m_{U0}	(0)	(0)	(0)	(0)	4	(0)

[a] Range of total peptide complex concentration used in experiment. [b] Stoichiometric factors of best fitting model. [c] Taken from M. Rabe et al.[50] [d] Calculated at 25 °C

Table S9. *Peptide helicity as determined by circular dichroism spectroscopy.*

Peptide		1_E	1_K	2_E	2_K	3_E	3_K	4_E	4_K
Acetyl[b]	%H[a]	7	10	21	13	5	22	29	11
	θ_{222} / θ_{208}	0.2	0.4	0.8	0.6	0.3	0.8	0.7	0.3
1% $Cpeg_4$	%H[a]	7	19	28	34	24	50	23	41
	θ_{222} / θ_{208}	0.1	0.3	0.3	0.5	0.5	0.7	0.4	0.5
2% $Cpeg_4$	%H[a]	5	16	16	37	24	39	20	28
	θ_{222} / θ_{208}	0.1	0.4	-0.4	0.6	-0.3	0.7	0.4	0.5
3% $Cpeg_4$	%H[a]	7	22	35	37	36	46	27	62
	θ_{222} / θ_{208}	0.2	0.5	2.1	0.7	-0.3	0.8	0.6	-18.2
4% $Cpeg_4$	%H[a]	7	21	34	50	42	53	33	63
	θ_{222} / θ_{208}	0.1	0.5	1.0	0.7	-0.5	1.0	0.5	-12.3

[a] Percentage a-helicity was calculated using the formula $[\theta]_{222}$=-39500(1-2.57/n) to obtain a 100% helicity value for an a-helical peptide of n residues.[62] [b] Measurements with N-acylated peptides, in PBS pH 7.4, without vesicles. [Total lipid] = 0.5 mM, PBS pH 7.4.*

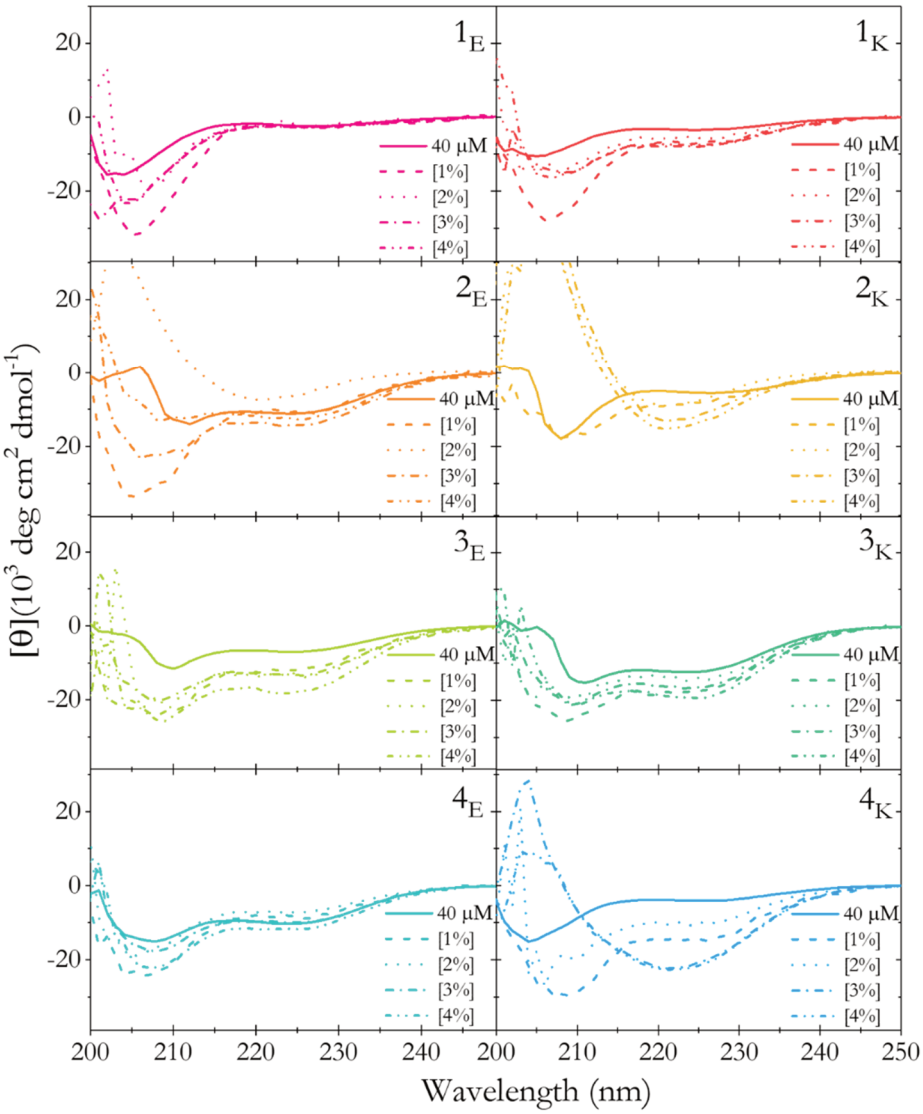

Figure S27. *CD spectra of peptides tethered to liposomes with increasing [Cpeg$_4$P]. [Total lipid] = 0.5 mM, in PBS pH 7.4 at 20 °C.*

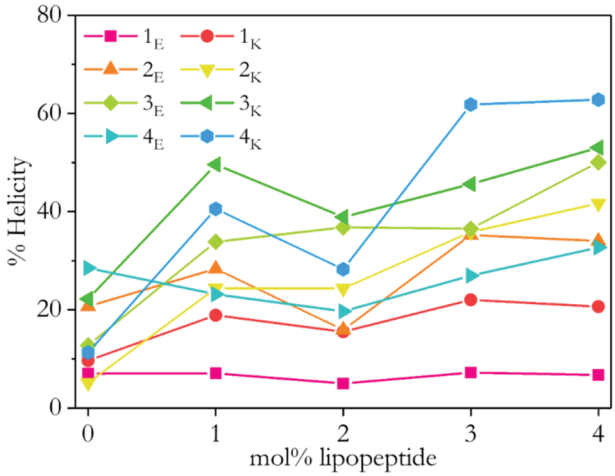

Figure S28. *Helicity of peptides tethered to liposomes with increasing [Cpeg$_4$P]. The first entry contains helicity of AcP-peptides. [AcP] = 200 µM; [total lipid] = 0.5 mM; with [Cpeg$_4$P] = 5, 10, 15, or 20 µM, in PBS pH 7.4 at 20 °C.*

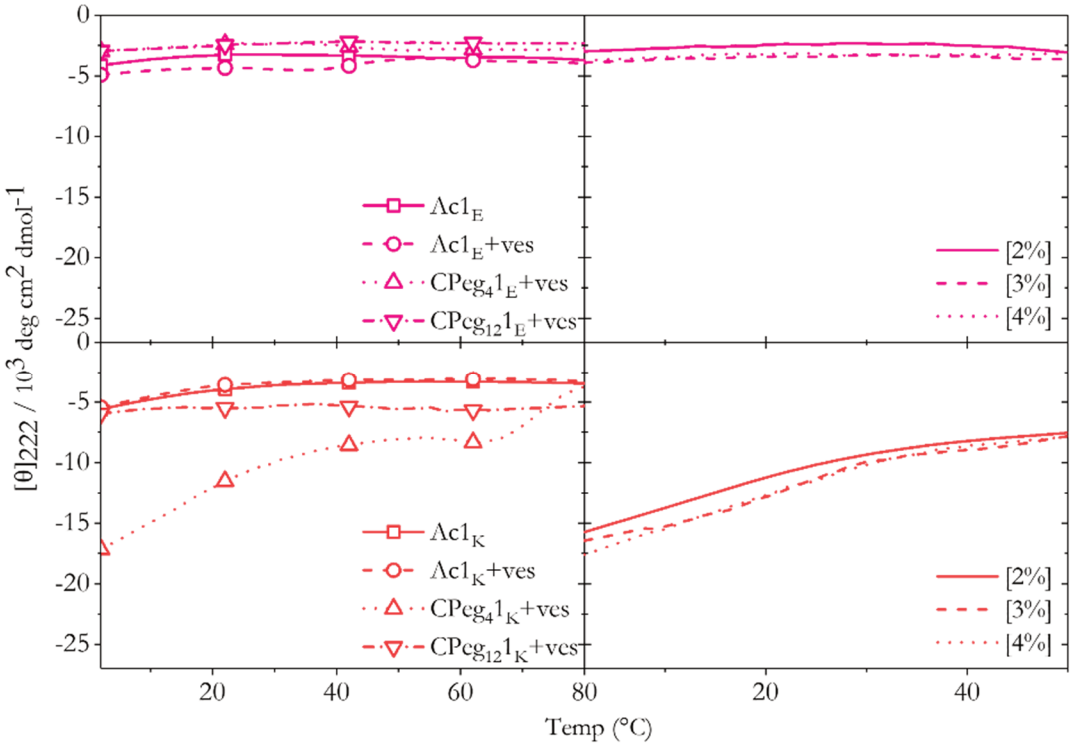

Figure S29. *Melting curves of 1_E and 1_K peptides. Left: with acylated peptides in the absence and presence of vesicles, and with lipopeptide decorated liposomes. Right: with increasing [Cpeg4P]. [Total lipid]+[AcP] = 1 mM+20 μM. [Total lipid]+[Cpeg4P] = 0.5 mM+ 5, 10, 15, or 20 μM, in PBS pH 7.4 at 20 °C.*

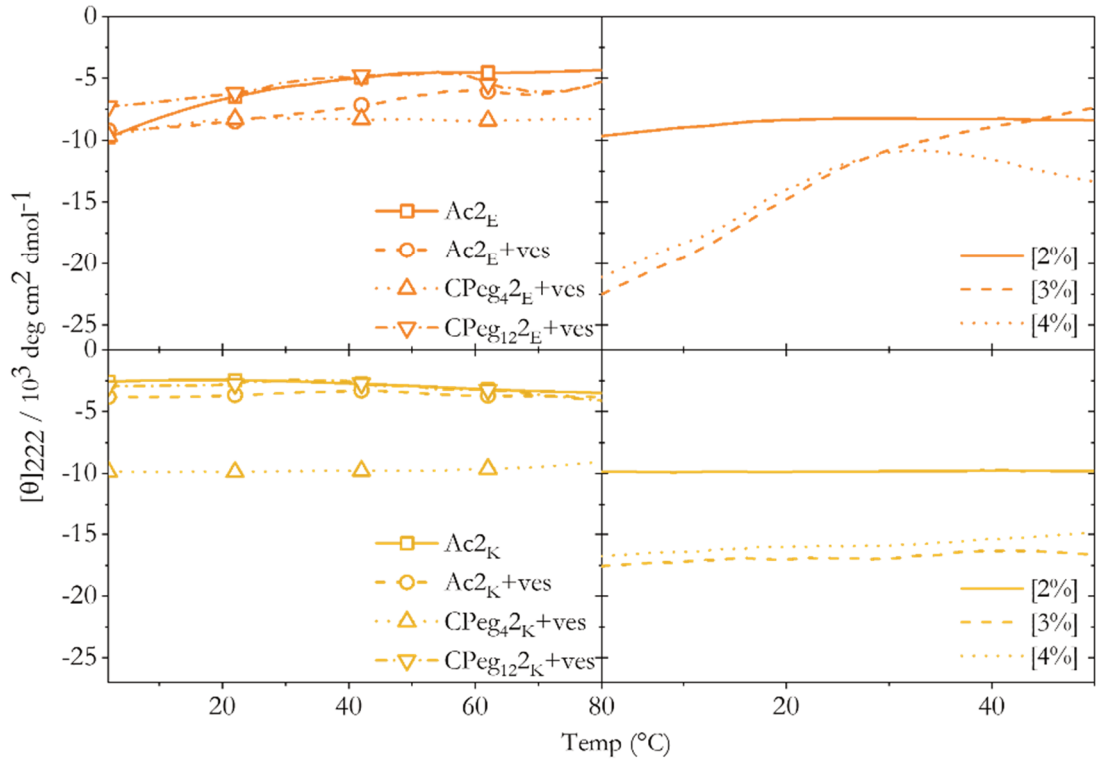

Figure S30. *Melting curves of 2_E and 2_K peptides. Left: with acylated peptides in the absence and presence of vesicles, and with lipopeptide decorated liposomes. Right: with increasing [Cpeg4P]. [Total lipid]+[AcP] = 1 mM+20 μM. [Total lipid]+[Cpeg4P] = 0.5 mM+ 5, 10, 15, or 20 μM, in PBS pH 7.4 at 20 °C.*

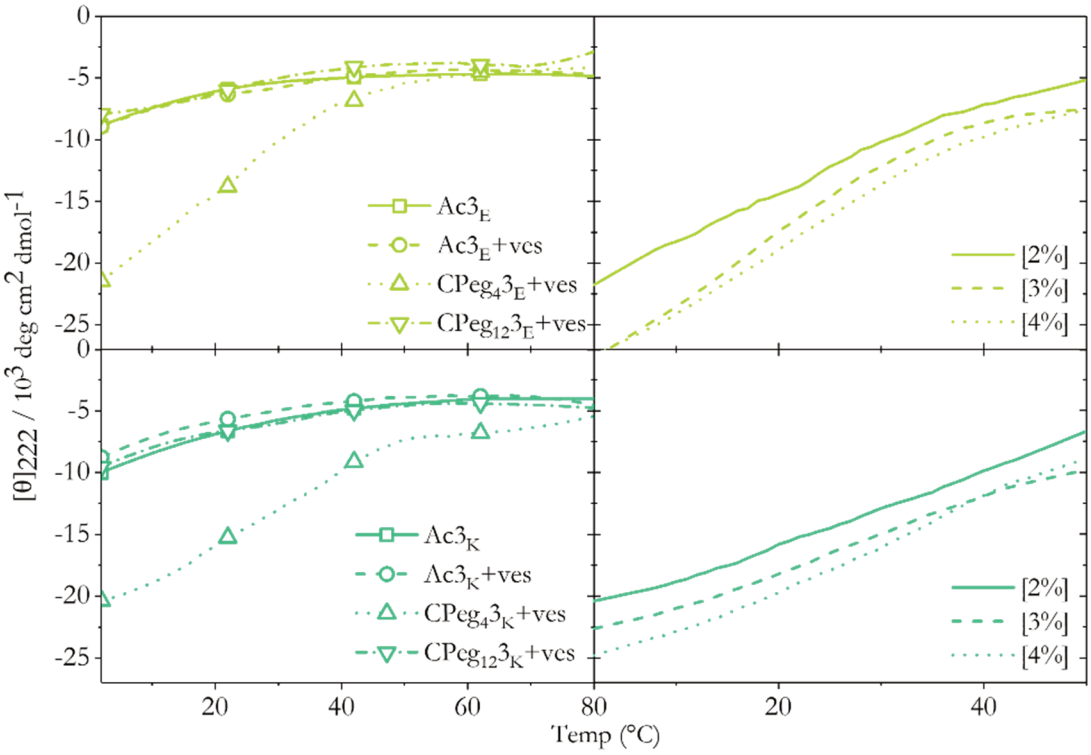

Figure S31. *Melting curves of 3_E and 3_K peptides. Left: with acylated peptides in the absence and presence of vesicles, and with lipopeptide decorated liposomes. Right: with increasing [Cpeg$_4$P]. [Total lipid]+[AcP] = 1 mM+20 μM. [Total lipid]+[Cpeg$_4$P] = 0.5 mM+ 5, 10, 15, or 20 μM, in PBS pH 7.4 at 20 °C.*

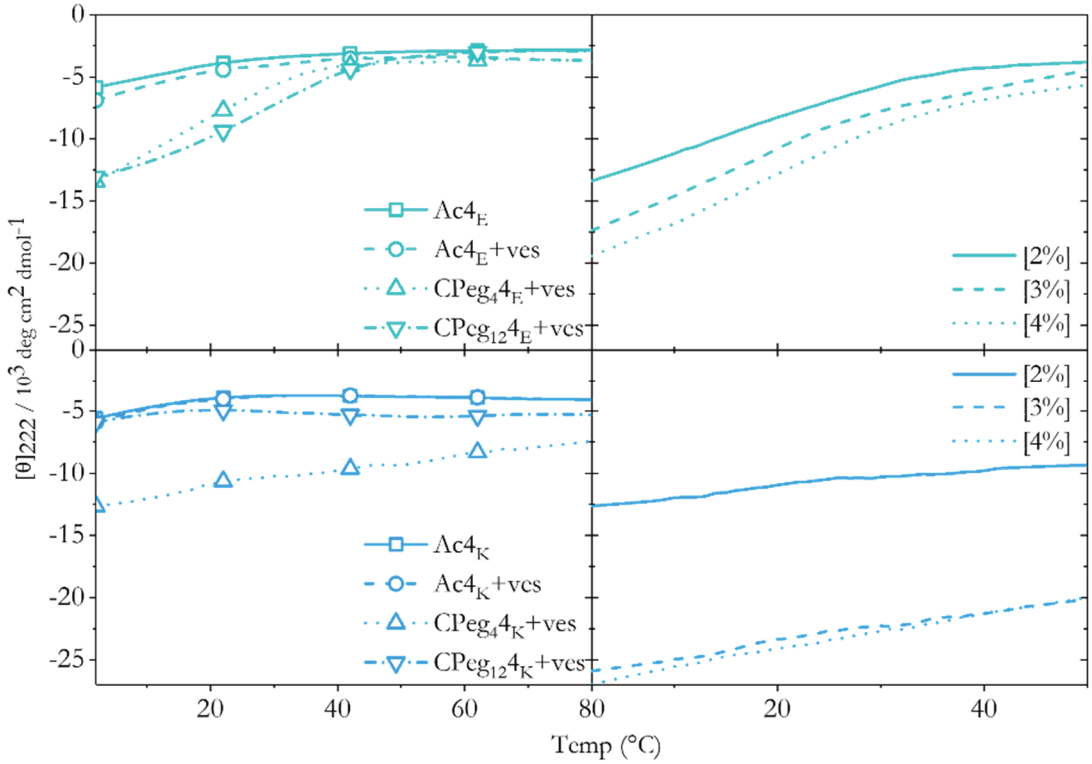

Figure S32. *Melting curves of 4_E and 4_K peptides. Left: with acylated peptides in the absence and presence of vesicles, and with lipopeptide decorated liposomes. Right: with increasing [Cpeg$_4$P]. [Total lipid]+[AcP] = 1 mM+20 μM. [Total lipid]+[Cpeg$_4$P] = 0.5 mM+ 5, 10, 15, or 20 μM, in PBS pH 7.4 at 20 °C.*

CONTENT MIXING

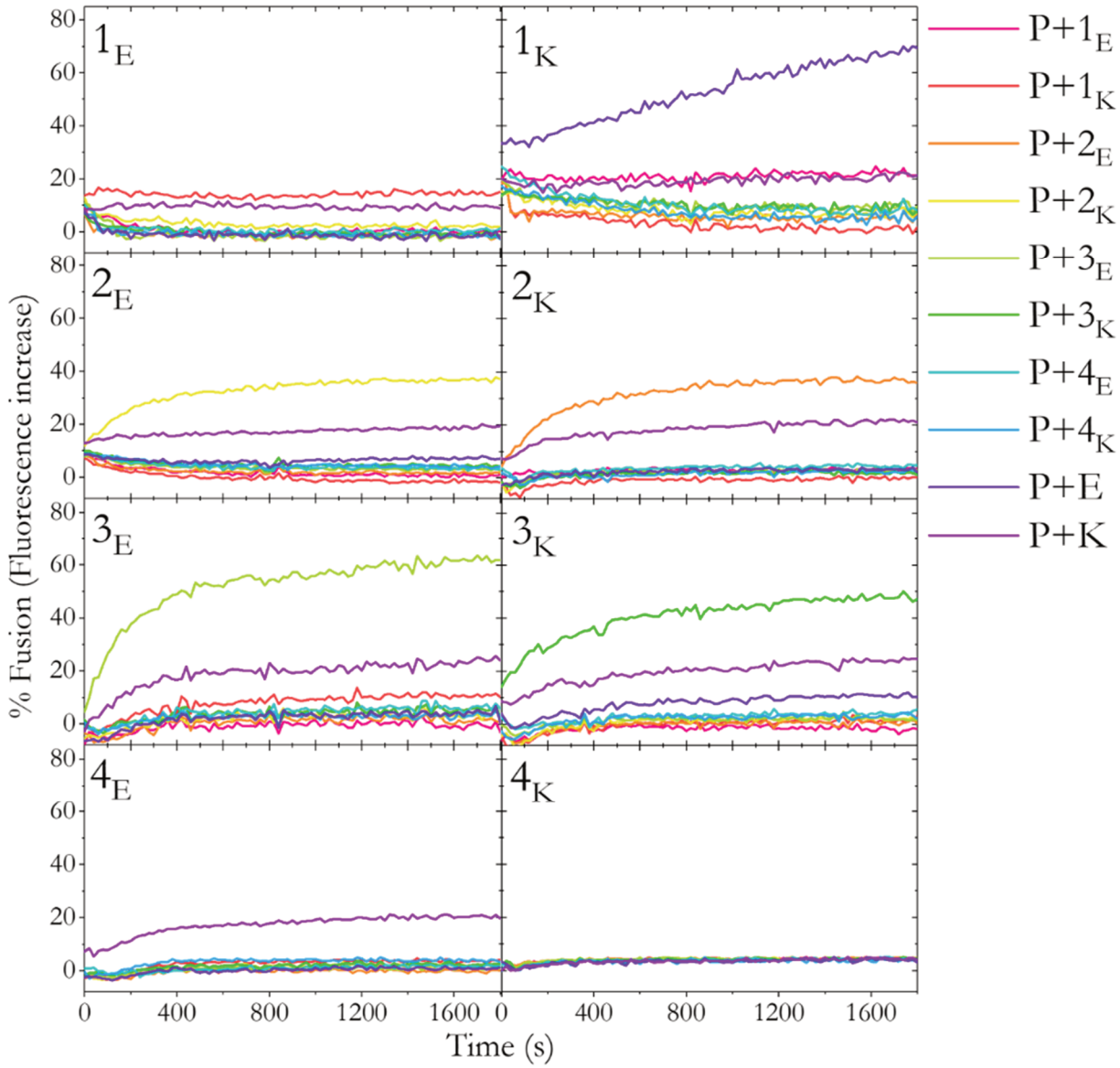

Figure S33. *Content mixing assay of liposomes functionalized with Cpeg$_4$P or Cpeg$_8$E/Cpeg$_8$K.. Results are ordered for liposomes functionalized with Cpeg$_4$P and loaded with Sulphorhodamine B, and all possible combinations of peptide functionalized liposomes were tested. [Total lipid] = 0.1 mM with 1 mol% lipopeptide in PBS pH 7.4 at 25 °C.*

REFERENCES

1. Stengel, G.; Zahn, R.; Hook, F., DNA-induced programmable fusion of phospholipid vesicles. *J. Am. Chem. Soc.* **2007,** *129* (31), 9584-9585.
2. Stengel, G.; Simonsson, L.; Campbell, R. A.; Hook, F., Determinants for membrane fusion induced by cholesterol-modified DNA zippers. *J. Phys. Chem. B* **2008,** *112* (28), 8264-8274.
3. Chan, Y. H.; van Lengerich, B.; Boxer, S. G., Lipid-anchored DNA mediates vesicle fusion as observed by lipid and content mixing. *Biointerphases* **2008,** *3* (2), FA17.
4. Chan, Y. H.; van Lengerich, B.; Boxer, S. G., Effects of linker sequences on vesicle fusion mediated by lipid-anchored DNA oligonucleotides. *Proc. Natl. Acad. Sci. U. S. A.* **2009,** *106* (4), 979-984.
5. Jakobsen, U.; Vogel, S., DNA-Controlled Assembly of Liposomes in Diagnostics. *Methods Enzymol.* **2009,** *464*, 233-248.
6. Ries, O.; Loffler, P. M. G.; Vogel, S., Convenient synthesis and application of versatile nucleic acid lipid membrane anchors in the assembly and fusion of liposomes. *Org. Biomol. Chem.* **2015,** *13* (37), 9673-9680.
7. Herrmann, A.; Meng, Z.; Yang, J.; Liu, Q.; de Vries, J. W.; Gruszka, A.; Rodriguez-Pulido, A.; Crielaard, B.; Kros, A., Efficient Fusion of Liposomes by Nucleobase Quadruple-Anchored DNA. *Chem. - Eur. J.* **2017**, DOI: 10.1002/chem.201701379.
8. Loffler, P. M. G.; Ries, O.; Rabe, A.; Okholm, A. H.; Thomsen, R. P.; Kjems, J.; Vogel, S., A DNA-Programmed Liposome Fusion Cascade. *Angewandte Chemie-International Edition* **2017,** *56* (43), 13228-13231.
9. Ries, O.; Loffler, P. M. G.; Rabe, A.; Malavan, J. J.; Vogel, S., Efficient liposome fusion mediated by lipid-nucleic acid conjugates. *Organic & Biomolecular Chemistry* **2017,** *15* (42), 8936-8945.
10. Lygina, A. S.; Meyenberg, K.; Jahn, R.; Diederichsen, U., Transmembrane Domain Peptide/Peptide Nucleic Acid Hybrid as a Model of a SNARE Protein in Vesicle Fusion. *Angew. Chem., Int. Ed.* **2011,** *50* (37), 8597-8601.
11. Kashiwada, A.; Matsuda, K.; Mizuno, T.; Tanaka, T., Construction of a pH-responsive artificial membrane fusion system by using designed coiled-coil polypeptides. *Chem. - Eur. J.* **2008,** *14* (24), 7343-7350.
12. Meyenberg, K.; Lygina, A. S.; van den Bogaart, G.; Jahn, R.; Diederichsen, U., SNARE derived peptide mimic inducing membrane fusion. *Chem. Commun. (Cambridge, U. K.)* **2011,** *47* (33), 9405-9407.
13. Rauschenberg, M.; Bomke, S.; Karst, U.; Ravoo, B. J., Dynamic Peptides as Biomimetic Carbohydrate Receptors. *Angew. Chem., Int. Ed.* **2010,** *49* (40), 7340-7345.
14. Richard, A.; Marchi-Artzner, V.; Lalloz, M. N.; Brienne, M. J.; Artzner, F.; Gulik-Krzywicki, T.; Guedeau-Boudeville, M. A.; Lehn, J. M., Fusogenic supramolecular vesicle systems induced by metal ion binding to amphiphilic ligands. *Proc. Natl. Acad. Sci. U. S. A.* **2004,** *101* (43), 15279-15284.
15. Gong, Y.; Luo, Y.; Bong, D., Membrane activation: selective vesicle fusion via small molecule recognition. *J. Am. Chem. Soc.* **2006,** *128* (45), 14430-14431.
16. Kashiwada, A.; Tsuboi, M.; Matsuda, K., Target-selective vesicle fusion induced by molecular recognition on lipid bilayers. *Chem. Commun.* **2009,** (6), 695-697.
17. Kashiwada, A.; Tsuboi, M.; Mizuno, T.; Nagasaki, T.; Matsuda, K., Target-selective vesicle fusion system with pH-selectivity and responsiveness. *Soft Matter* **2009,** *5* (23), 4719-4725.
18. Kashiwada, A.; Tsuboi, M.; Takamura, N.; Brandenburg, E.; Matsuda, K.; Koksch, B., Design and Characterization of Endosomal-pH-Responsive Coiled-coils for

Constructing an Artificial Membrane Fusion System. *Chem. - Eur. J.* **2011,** *17* (22), 6179-6186.
19. Marchi-Artzner, V.; Gulik-Krzywicki, T.; Guedeau-Boudeville, M. A.; Gosse, C.; Sanderson, J. M.; Dedieu, J. C.; Lehn, J. M., Selective adhesion, lipid exchange and membrane-fusion processes between vesicles of various sizes bearing complementary molecular recognition groups. *ChemPhysChem* **2001,** *2* (6), 367-376.
20. Ma, M. M.; Bong, D., Controlled Fusion of Synthetic Lipid Membrane Vesicles. *Acc. Chem. Res.* **2013,** *46* (12), 2988-2997.
21. Marsden, H. R.; Tomatsu, I.; Kros, A., Model systems for membrane fusion. *Chem. Soc. Rev.* **2011,** *40* (3), 1572-85.
22. Chen, Y. A.; Scheller, R. H., SNARE-mediated membrane fusion. *Nat. Rev. Mol. Cell Biol.* **2001,** *2* (2), 98-106.
23. Jahn, R.; Scheller, R. H., SNAREs--engines for membrane fusion. *Nat. Rev. Mol. Cell Biol.* **2006,** *7* (9), 631-43.
24. Jena, B. P., Membrane fusion: role of SNAREs and calcium. *Protein Pept. Lett.* **2009,** *16* (7), 712-7.
25. Sudhof, T. C.; Rothman, J. E., Membrane Fusion: Grappling with SNARE and SM Proteins. *Science* **2009,** *323* (5913), 474-477.
26. Woolfson, D. N., The design of coiled-coil structures and assemblies. *Fibrous Proteins: Coiled-Coils, Collagen and Elastomers* **2005,** *70*, 79-+.
27. Ogihara, N. L.; Weiss, M. S.; Degrado, W. F.; Eisenberg, D., The crystal structure of the designed trimeric coiled-coil coil-V(a)L(d): Implications for engineering crystals and supramolecular assemblies. *Protein Sci.* **1997,** *6* (1), 80-88.
28. Fletcher, J. M.; Boyle, A. L.; Bruning, M.; Bartlett, G. J.; Vincent, T. L.; Zaccai, N. R.; Armstrong, C. T.; Bromley, E. H. C.; Booth, P. J.; Brady, R. L.; Thomson, A. R.; Woolfson, D. N., A Basis Set of de Novo Coiled-Coil Peptide Oligomers for Rational Protein Design and Synthetic Biology. *ACS Synth. Biol.* **2012,** *1* (6), 240-250.
29. Mende-Thomas, F.; Boyle, A. L.; Armstrong, C. T.; Woolfson, D. N., De novo designed heterodimeric coiled-coils - Useful tools for the development of new biomaterials. *J. Pept. Sci.* **2012,** *18*, S27-S28.
30. Thomas, F.; Boyle, A. L.; Burton, A. J.; Woolfson, D. N., A Set of de Novo Designed Parallel Heterodimeric Coiled-coils with Quantified Dissociation Constants in the Micromolar to Sub-nanomolar Regime. *J. Am. Chem. Soc.* **2013,** *135* (13), 5161-5166.
31. Wood, C. W.; Bruning, M.; Ibarra, A. A.; Bartlett, G. J.; Thomson, A. R.; Sessions, R. B.; Brady, R. L.; Woolfson, D. N., CCBuilder: an interactive web-based tool for building, designing and assessing coiled-coil protein assemblies. *Bioinformatics* **2014,** *30* (21), 3029-3035.
32. Gradisar, H.; Jerala, R., De novo design of orthogonal peptide pairs forming parallel coiled-coil heterodimers. *J. Pept. Sci.* **2011,** *17* (2), 100-106.
33. Bromley, E. H. C.; Sessions, R. B.; Thomson, A. R.; Woolfson, D. N., Designed alpha-Helical Tectons for Constructing Multicomponent Synthetic Biological Systems. *J. Am. Chem. Soc.* **2009,** *131* (3), 928-+.
34. Diss, M. L.; Kennan, A. J., Orthogonal recognition in dimeric coiled-coils via buried polar-group modulation. *J. Am. Chem. Soc.* **2008,** *130* (4), 1321-1327.
35. Reinke, A. W.; Grant, R. A.; Keating, A. E., A Synthetic Coiled-Coil Interactome Provides Heterospecific Modules for Molecular Engineering. *J. Am. Chem. Soc.* **2010,** *132* (17), 6025-6031.
36. Skyttner, C.; Enander, K.; Aronsson, C.; Aili, D., Tuning Liposome Membrane Permeability by Competitive Coiled-coil Heterodimerization and Heterodimer Exchange. *Langmuir* **2018,** *34* (22), 6529-6537.

37. Aronsson, C.; Danmark, S.; Zhou, F.; Oberg, P.; Enander, K.; Su, H. B.; Aili, D., Self-sorting heterodimeric coiled-coil peptides with defined and tuneable self-assembly properties. *Scientific Reports* **2015,** *5*.
38. Ladokhin, A. S.; White, S. H., Folding of amphipathic alpha-helices on membranes: Energetics of helix formation by melittin. *J. Mol. Biol.* **1999,** *285* (4), 1363-1369.
39. Almeida, P. F.; Ladokhin, A. S.; White, S. H., Hydrogen-bond energetics drive helix formation in membrane interfaces. *Biochim. Biophys. Acta, Biomembr.* **2012,** *1818* (2), 178-182.
40. Rabe, M.; Aisenbrey, C.; Pluhackova, K.; de Wert, V.; Boyle, A. L.; Bruggeman, D. F.; Kirsch, S. A.; Bockmann, R. A.; Kros, A.; Raap, J.; Bechinger, B., A Coiled-Coil Peptide Shaping Lipid Bilayers upon Fusion. *Biophys. J.* **2016,** *111* (10), 2162-2175.
41. Strandberg, E.; Killian, J. A., Snorkeling of lysine side chains in transmembrane helices: how easy can it get? *FEBS Lett.* **2003,** *544* (1-3), 69-73.
42. Mishra, V. K.; Palgunachari, M. N., Interaction of model class A(1), class A(2) and class Y amphipathic helical peptides with membranes. *Biochemistry* **1996,** *35* (34), 11210-11220.
43. Segrest, J. P.; Deloof, H.; Dohlman, J. G.; Brouillette, C. G.; Anantharamaiah, G. M., Amphipathic Helix Motif - Classes and Properties. *Proteins: Struct., Funct., Genet.* **1990,** *8* (2), 103-117.
44. Drin, G.; Antonny, B., Amphipathic helices and membrane curvature. *Febs Lett.* **2010,** *584* (9), 1840-1847.
45. Rabe, M.; Schwieger, C.; Zope, H. R.; Versluis, F.; Kros, A., Membrane Interactions of Fusogenic Coiled-Coil Peptides: Implications for Lipopeptide Mediated Vesicle Fusion. *Langmuir* **2014,** *30* (26), 7724-7735.
46. Daudey, G. A.; Zope, H. R.; Voskuhl, J.; Kros, A.; Boyle, A. L., Membrane-Fusogen Distance Is Critical for Efficient Coiled-Coil-Peptide-Mediated Liposome Fusion. *Langmuir* **2017,** *33* (43), 12443-12452.
47. Yang, J.; Bahreman, A.; Daudey, G.; Bussmann, J.; Olsthoorn, R. C.; Kros, A., Drug Delivery via Cell Membrane Fusion Using Lipopeptide Modified Liposomes. *ACS Cent. Sci.* **2016,** *2* (9), 621-630.
48. Greenfield, N. J., Using circular dichroism spectra to estimate protein secondary structure. *Nat. Protoc.* **2006,** *1* (6), 2876-2890.
49. Greenfield, N. J., Methods to estimate the conformation of proteins and polypeptides from circular dichroism data. *Anal. Biochem.* **1996,** *235* (1), 1-10.
50. Rabe, M.; Boyle, A.; Zope, H. R.; Versluis, F.; Kros, A., Determination of Oligomeric States of Peptide Complexes Using Thermal Unfolding Curves. *Biopolymers* **2015,** *104* (2), 65-72.
51. Rabe, M.; Zope, H. R.; Kros, A., Interplay between Lipid Interaction and Homo-coiling of Membrane-Tethered Coiled-Coil Peptides. *Langmuir* **2015,** *31* (36), 9953-9964.
52. Kyoung, M.; Srivastava, A.; Zhang, Y. X.; Diao, J. J.; Vrljic, M.; Grob, P.; Nogales, E.; Chu, S.; Brunger, A. T., In vitro system capable of differentiating fast Ca2+-triggered content mixing from lipid exchange for mechanistic studies of neurotransmitter release. *Proc. Natl. Acad. Sci. U. S. A.* **2011,** *108* (29), E04-E13.
53. Stratton, B. S.; Warner, J. M.; Wu, Z. Y.; Nikolaus, J.; Wei, G.; Wagnon, E.; Baddeley, D.; Karatekin, E.; O'Shaughnessy, B., Cholesterol Increases the Openness of SNARE-Mediated Flickering Fusion Pores. *Biophys. J.* **2016,** *110* (7), 1538-1550.
54. Han, J.; Pluhackova, K.; Bockmann, R. A., The Multifaceted Role of SNARE Proteins in Membrane Fusion. *Front. Membr. Physiol. Membr. Biophys.* **2017,** *8*, 5.
55. Rizo, J.; Xu, J., The Synaptic Vesicle Release Machinery. *Annu. Rev. Biophys.* **2015,** *44*, 339-67.

56. Yang, J.; Shimada, Y.; Olsthoorn, R. C. L.; Snaar-Jagalska, B. E.; Spaink, H. P.; Kros, A., Application of Coiled-coil Peptides in Liposomal Anticancer Drug Delivery Using a Zebrafish Xenograft Model. *ACS Nano* **2016,** *10* (8), 7428-7435.
57. Zope, H. R.; Versluis, F.; Ordas, A.; Voskuhl, J.; Spaink, H. P.; Kros, A., In vitro and in vivo supramolecular modification of biomembranes using a lipidated coiled-coil motif. *Angew. Chem., Int. Ed.* **2013,** *52* (52), 14247-51.
58. Cubberley, M. S.; Iverson, B. L., (1)H NMR investigation of solvent effects in aromatic stacking interactions. *J. Am. Chem. Soc.* **2001,** *123* (31), 7560-7563.
59. Shirude, P. S.; Kumar, V. A.; Ganesh, K. N., BisPNA targeting to DNA: Effect of neutral loop on DNA duplex strand invasion by aepPNA-N7G/aepPNA-C substituted peptide nucleic acids. *Eur. J. Org. Chem.* **2005,** (24), 5207-5215.
60. Sun, Q.; Cai, S.; Peterson, B. R., Practical Synthesis of 3 beta-Amino-5-cholestene and Related 3 beta-Halides Involving i-Steroid and Retro-i-Steroid Rearrangements. *Org. Lett.* **2009,** *11* (3), 567-570.
61. Marsden, H. R.; Elbers, N. A.; Bomans, P. H. H.; Sommerdijk, N.; Kros, A., A Reduced SNARE Model for Membrane Fusion. *Angew. Chem., Int. Ed.* **2009,** *48* (13), 2330-2333.
62. Lacroix, E.; Viguera, A. R.; Serrano, L., Elucidating the folding problem of alpha-helices: local motifs, long-range electrostatics, ionic-strength dependence and prediction of NMR parameters. *J Mol Biol* **1998,** *284* (1), 173-91.
63. Oshea, E. K.; Lumb, K. J.; Kim, P. S., Peptide Velcro - Design of a Heterodimeric Coiled-Coil. *Curr. Biol.* **1993,** *3* (10), 658-667.
64. Kozlowski, L. P., IPC - Isoelectric Point Calculator. *Biology Direct* **2016,** *11*.